U. of Iowa 67-29

Geomagnetically Trapped Alpha Particles*

by

S. M. Krimigis and J. A. Van Allen

Department of Physics and Astronomy
University of Iowa
Iowa City, Iowa

July 1967

*Research supported in part by National Aeronautics and Space Administration Grant NsG 233-62 and Contract NAS1-2973 with the Langley Research Center and by Office of Naval Research Contract Nonr 1509(06).

ABSTRACT

The observations reported herein were made with the University of Iowa Injun IV satellite which was launched on 21 November 1964 into a nearly polar orbit of 81° inclination with initial apogee and perigee altitudes of 2502 and 527 kilometers, respectively. It carried a 25 micron thick, totally depleted silicon surface barrier detector with four electronic discrimination levels. The two lower levels are sensitive to protons $0.52 \leq E_p \leq 4.0$ MeV and $0.90 \leq E_p \leq 1.8$ MeV, respectively. The two upper levels are sensitive only to nuclei heavier than deuterons and, specifically, are sensitive to alpha particles $2.09 \leq E_\alpha \leq 15$ MeV and $3.89 \leq E_\alpha \leq 7$ MeV, respectively. Study of the available data up to 17 April 1965 leads to the following conclusions:

(a) The presence of geomagnetically trapped alpha particles is established.

(b) At constant $|\vec{B}| \approx 0.19$ gauss the maximum intensity perpendicular to $\vec{B}$ occurs at L = 3.1. The absolute directional intensity there is

$$j_\alpha (E_\alpha > 2.09 \text{ MeV}) = 28 \ (\text{cm}^2 \text{ sec sr})^{-1} \text{ and}$$

$$j_\alpha (E_\alpha > 3.89 \text{ MeV}) = 4.5 \ (\text{cm}^2 \text{ sec sr})^{-1} .$$

(c) At this outer zone maximum, the ratio of the directional intensities of alpha particles and of protons, both integrated above the common value $\mathcal{E}_\alpha = \mathcal{E}_p = 0.52$ MeV/nucleon, is

$$j_\alpha/j_p = (2.3 \pm 0.2) \times 10^{-4} .$$

(d) A variety of considerations, no one of which is decisive, suggest that the most physically significant form of the spectra of alpha particles and protons may be an exponential one in terms of energy/nucleon.

(e) It appears conceivable that the observed ratio j_α/j_p may be reconcilable with a solar-wind-source of outer zone protons and alpha particles although this ratio is significantly less than that predicted from diffusion theory with known loss processes taken into account.

(f) The distribution of outer zone alpha particles was changed markedly after the magnetic storm of 18 April 1965 and the intensity peak moving inward from L = 3.1 to L = 2.9.

(g) Trapped alpha particles in the inner zone are apparently due to a different source than that for those in the outer zone.

1. INTRODUCTION AND SUMMARY

Studies over the past several years have shown that the geomagnetically trapped radiation consists dominantly of protons and electrons having energies from a few eV to many MeV. Several investigators have searched for particles heavier than protons using nuclear emulsions. Freden and White [1960] identified five triton tracks in the energy range 126 to 200 MeV and one deuteron track in recovered emulsions flown on two rockets through the lower edge of the inner radiation zone. The total number of proton tracks in a comparable energy range was 496. In two similar flights of emulsions Heckman and Armstrong [1962] found five deuteron tracks in the energy range 93 to 133 MeV and no triton tracks out of a total of 788 tracks studied, the other 783 tracks being identified as due to protons. Neither of these groups reported the presence of helium nuclei, although their absence was not considered surprising, in view of the high energy thresholds of the detectors for alpha particles and the limited statistical sample. Heckman and Armstrong set an upper limit of 1×10^{-3} for the intensity ratio of alpha particles to protons in the energy interval 125 to 185 MeV. In a later emulsion experiment Naugle and Kniffen [1963] placed an upper limit of 6×10^{-3} for intensity ratio of all particles heavier than protons to protons in the energy interval 12 to

30 MeV/nucleon ($E_\alpha > 50$ MeV), at altitudes up to 2000 km in the region $1.45 < L < 1.85$.

All of the results quoted so far were obtained for $L < 1.85$, i.e., in the inner zone. More recently Fenton [1967] has searched for alpha particles in the region $1.6 \leq L \leq 3.3$ using a solid state detector telescope on OGO-I. On the basis of what he judges to be an essentially null result, he suggests an upper limit for the alpha particle to proton intensity ratio in the interval 26 to 85 MeV/nucleon of 6.7×10^{-4}.

In this paper we report the results of an extensive search for geomagnetically trapped nuclei heavier than deuterons in the energy range $0.52 \leq E \leq 4$ MeV/nucleon, an energy region which is roughly two orders of magnitude below the regions previously investigated. Preliminary results of this experiment were reported earlier [Van Allen and Krimigis, 1965; Krimigis and Van Allen, 1966; Krimigis, Van Allen, and Armstrong, 1967]. It is found that (a) trapped nuclei heavier than protons are present with measurable intensity in the earth's radiation zones; (b) the maximum intensity of such particles occurs at $L \simeq 3.1$; (c) the observed particles are most reasonably identified as alpha particles; (d) the integral intensity ratio j_α/j_p for energies >0.52 MeV/nucleon is $\sim 2 \times 10^{-4}$ at $L \simeq 3.1$ and $|\vec{B}| = 0.19$ gauss, a result independent of the respective energy spectra; and (e) some information on the α-particle energy spectrum is obtained.

The significance of these observations lies in the fact that, although the intensity and energy spectrum of trapped protons $E_p \gtrsim 30$ MeV can be reasonably accounted for on the basis of the cosmic ray albedo neutron hypothesis, protons of energy below 30 MeV and down to 0.1 MeV or less cannot possibly be attributed to the albedo-neutron source. Such lower energy protons are commonly thought to be due to injection of solar wind particles into the magnetosphere and subsequent acceleration and diffusion across magnetic shells therein. Other conjectures attribute their presence (a) to the direct magnetospheric capture of solar cosmic rays; (b) to the decay of neutrons produced in the polar cap atmosphere by solar cosmic rays; and (c) to the in situ acceleration of particles which are a component of the earth's own exosphere.

Thus, the special motivation for study of trapped nuclei having $Z \geq 2$ is to provide a set of parameters on one or more "tracer" components of the radiation belts for testing the validity of hypotheses on their origin and on the origin of the much more abundant proton component.

2. DESCRIPTION OF THE DETECTOR

The observations reported herein were obtained with the University of Iowa satellite Injun IV. The relevant detector is a totally depleted silicon one of the surface barrier kind in the form of a thin circular disc, whose thickness is 25 microns and whose frontal area is 1.75 ± 0.2 mm^2 (Nuclear Diodes, Inc.). The detector is located inside a conical collimator with a full vertex angle of 40° and is otherwise sheilded by a minimum of 10.2 g/cm^2 of brass, which corresponds to the range of 95 MeV protons (Figure 1). Four electronic discrimination levels are provided. The first two (channels A and B) are sensitive to protons and heavier nuclei and the last two (channels C and D) are sensitive only to particles heavier than deuterons (Table 1).

The scheme for energy discrimination is illustrated in Figure 2. The maximum energy that an axially incident proton can deposit in the detector is 1.3 MeV. Since the energy needed to trigger channel C is 1.8 MeV, only particles that are heavier than protons are counted in channel C. An examination of the range-energy curves for deuterons, tritons, He^3, and He^4 shows that channel C will clearly count He^3 and He^4 (as well as nuclei having greater Z), may just barely count tritons in a narrow energy range, but will <u>not</u> count deuterons. Similarly the energy

that must be deposited in the detector to trigger channel D is 3.7 MeV; hence only He^3, He^4, and heavier nuclei can be counted by this channel.

The calibration method used is identical to that described in detail elsewhere for similar detectors from this laboratory [Krimigis and Armstrong, 1966]. In addition, a special test run was made on the Naval Research Laboratory's Van de Graaff accelerator (courtesy of E. Wolicki) in order to determine the efficiency of channels C and D for protons whose total energy was sufficient to trigger these channels, if for some spurious or unsuspected reason these protons were able to deposit enough energy in the detector to actually do so. The detector, connected to flight electronics, was placed in a beam of 1.8 MeV protons and the outputs of channels A (sensitive to protons) and C were recorded. It was found that the efficiency of channel C for counting protons of the above energy, given by C/A, was 3×10^{-4} with an accuracy of 10%. The experiment was repeated at proton energies of 1.9, 2.05, and 3.57 MeV. The efficiency remained approximately constant as a function of energy at the value of $\sim 3 \times 10^{-4}$. The constancy of the efficiency with energy indicates that the counts seen in channel C may have been due to stray alpha particles or heavier nuclei that had entered the selecting magnet in the accelerator with the same momentum/unit charge as the protons. In a typical Van de Graaff accelerator, the "purity"

of the proton beam is usually no better than 1 part in 10^3 [R. R. Carlson and E. Norbeck, private communication].

The interpretation of the channel C counts as due to stray alpha particles is supported by the fact that a subsequent experiment using the flight spare unit gave an efficiency of $\sim 5 \times 10^{-5}$, nearly a factor of ten less than that found for the flight unit. (The two units were accurately similar.) It was established that during the three months previous to the performance of the second experiment, no helium gas had been used in the Van de Graaff [E. Wolicki, private communication] so that the proton beam was presumably more pure. The foregoing supports the belief that the proton efficiency of channel C may be considerably less than 3×10^{-4}; nonetheless we will adopt this number as an upper limit for the purposes of this paper.

The proton efficiency of channel D, measured in a similar manner as that of C, was found to be $\lesssim 1 \times 10^{-5}$.

Knowledge of the in-flight operation of the detector and the associated electronics is obtained by means of a permanently mounted $_{95}Am^{241}$ source of α-particles. The source was gold-plated to obtain a falling spectrum between 0.5 MeV and 3.9 MeV and thus to provide an in-flight measure of the stability of the system and

in particular that of the effective discrimination levels. For example, a 40% increase in the background rate of detector C results from lowering its discrimination level from 1.8 to 1.4 MeV. Yet no departure of its in-flight background rate (over the polar caps) by as much as $\pm$ 5% has been observed during the period of the observations on which the present paper is based. The total depletion of the detector and a strong developmental effort on making the entire system insensitive to variations in temperature and supply voltage contribute to the stability and trustworthiness of the detector.

None of the channels A, B, C, and D is sensitive to galactic cosmic rays.

3. DATA ANALYSIS

The Injun IV satellite was launched on 21 November 1964 into a nearly polar orbit of 81° inclination, with initial apogee altitude of 2502 kilometers and perigee altitude of 527 kilometers. The satellite is equipped with a permanent magnet and energy-dissipating hysteresis rods so that it will maintain a particular axis continuously aligned with the local geomagnetic field vector. Due to a large initial angular velocity at launch and weak damping, magnetic alignment did not occur until the latter part of February 1965. Thereafter, the axis of the detector collimator was maintained continuously perpendicular ($\pm 10°$) to the local magnetic field vector so that the detector was receiving particles whose pitch angles were $90° \pm 30°$. The primary body of data reported in this paper was obtained during the period 1 March to 17 April 1965. Auxiliary data on angular distributions were obtained during the tumbling period in December 1964 and January-February 1965. These auxiliary observations are of importance in establishing the validity of our interpretation of detector responses.

All telemetered data from the satellite are merged with the orbit parameters $|\vec{B}|$, L, and local time and subsequently sorted into subsets specified by selected ranges of $|\vec{B}|$ and L. The L interval used in this study is 0.1 and the $|\vec{B}|$ interval

0.02 gauss. For a given L interval, the directional intensity perpendicular to $\vec{B}$ is plotted as a function of $|\vec{B}|$. From a family of such plots, a graphical display is made of constant intensity contours in $|\vec{B}|$, L space.

4. OBSERVATIONS

In Figure 3, the counting rates of channels C and D as a function of L are shown for a constant value of $|\vec{B}|$. The data are averaged over the time period 1 March to 17 April 1965. The latter date was chosen as a cutoff date because a severe magnetic storm which occurred on that day perturbed the distributions of both protons and heavier particles [Krimigis, 1967a]. The counting rates due to the inflight source are indicated by the dashed lines. The essential features of the figure may be summarized as follows: (a) The principal maximum occurs at $L = 3.1 \pm 0.1$ for both channels C and D. (b) The counting rates are roughly constant from $L = 1.3$ to $L = 2.6$ but rise sharply in the L interval 2.6 to 3.1. (c) The ratio C/D has a relative minimum at the point of maximum counting rate and increases significantly on either side, although it remains constant (within statistical uncertainty) in the inner zone. (d) The counting rates are indistinguishable from background for $L \gtrsim 4.3$ for C and for $L \gtrsim 3.9$ for D. The threshold counting rates correspond to intensities of 4.5 $(cm^2 \text{ sec sr})^{-1}$ and 1.5 $(cm^2 \text{ sec sr})^{-1}$ for channels C and D, respectively. In Figure 4 the counting rate vs L profile at a constant $|\vec{B}|$ is shown for channel A, responding to protons in the energy

interval $0.52 \leq E_p \leq 4$ MeV, and for channel C ($0.52 \leq E_\alpha \leq 4$ MeV/nucleon). It is seen that, although the point of maximum intensity occurs at the same L value for both A and C, there exist important differences in the nature of the two profiles. The counting rate of channel A increases smoothly in the L interval 1.1 to 2.6 by a factor of over 10^3, whereas the counting rate of C changes by less than a factor of two in the L interval 1.3 to 2.6. However, in the L range 2.6 to 4.2 the ratio A/C is approximately constant. Thus it appears that the responses of channels C and D may be divided into two distinctively different regions namely $L \leq 2.6$ (referred to henceforth as the inner zone, in rough analogy to the usual terminology) and $L \geq 2.6$ (the outer zone). The validity of this impression is further supported by plots of constant intensity coutours in $|\vec{B}|$, L space (Figures 5 and 6). It is seen that at constant $|\vec{B}|$, both channels C and D exhibit relative maxima at $L \simeq 2.0$. The principal maxima occur at $L \sim 3.1$.

Thus, the data suggest that the responses of detectors C and D are due to different causes in the two different regions, the inner and outer zones.

It is important to note that the distributions of 0.5 MeV and 0.9 MeV protons obtained from channels A and B of the same detector do not exhibit such "double-peaked" intensity profiles [Krimigis, 1967b].

The nature of the responses of C and D in the two different regions is now examined further in two ways:

(a) During the magnetically aligned period, the $|\vec{B}|$ dependence of the counting rates at constant L is plotted.

(b) During the period before the satellite was magnetically aligned, the angular dependence of the counting rates at constant L and constant $|\vec{B}|$ is plotted, i.e., the dependence on the angle between $\vec{B}$ and the axis of the detector. The attitude of the satellite with respect to $\vec{B}$ is measured continuously by a system of Schonstedt magnetometers.

A. Inner Zone

Figure 7 shows the counting rates of channels A (protons having $0.52 \leq E_p \leq 4.0$ MeV), B ($0.90 \leq E_p \leq 1.8$ MeV), and C and D as a function of $|\vec{B}|$ for $L = 1.55 \pm 0.15$. The counting rates of C and D decrease monotonically with increasing $|\vec{B}|$ in a manner generally similar to the counting rates of A and B. The similarity is further enhanced when the net counting rates are plotted (i.e., after subtraction of the appropriate rates of the in-flight calibrating source).

Figure 8 shows the angular dependence of the counting rate of channel C, averaged over the L interval 1.3 to 1.7 and the $|\vec{B}|$ interval 0.10 to 0.20. Symbol φ denotes the angle between the collimator axis of the detector and the local magnetic field vector. This angle is defined as equal to zero when the collimator axis is parallel

the $|\vec{B}|$ vector in the northern hemisphere, i.e., the detector is pointing toward the earth. The counting rate curve appears to have two distinct components, one having a maximum at $\varphi = 90°$, with a full width at half maximum of $\sim 60°$, and a second having a maximum at $\varphi = 0°$ and probably also at 180°. Most of the data on which Figure 8 is based was distributed more-or-less uniformly over the $|\vec{B}|$ range specified. However, the point at $\varphi = 10°$ was based mainly on data in the low end of the range and may therefore be somewhat high (cf. Figure 7). (The counting rate of channel D is too low to permit a significant angular analysis.)

The significance of Figures 7 and 8 is developed in a later section.

B. Outer Zone

Figure 9 shows the $|\vec{B}|$ dependence of the counting rates of detectors A, B, C, and D for a constant L at the counting rate maximum in the outer zone (cf. Figures 3 and 4). Again, the functional similarity of the four curves is evident. Figure 10 shows the φ dependence of the counting rate of channel C at constant L and $|\vec{B}|$ near the outer zone maximum. This curve is similar to that of Figure 8 in that it shows a strong maximum at $\varphi = 90°$ but it is decidedly dissimilar for $\varphi < 50°$. Specifically, there is a complete absence of counts for $30° < \varphi < 0°$, despite the fact that this angular region was sampled repeatedly.

5. CONSIDERATION OF SPURIOUS EFFECTS

The data shown in section 4 establish that the counting rates of C and D are due to geomagnetically trapped particles and not to galactic cosmic rays, for example.

As shown in Table 1 and discussed in section 2, channel C responds ideally, only to tritons and heavier nuclei, and channel D only to He^3 and heavier nuclei.

Nonetheless, there are many physical processes which may conceivably cause counts in channels C and D and thus invalidate a simple minded interpretation. After a preliminary sifting of all such processes that we have been able to think of, we have arrived at the following list as worthy of detailed quantitative assessment:

(1) Proton pulse pile-up.

(2) Transverse penetration of the detector by high energy protons ($E_p \geq 95$ MeV).

(3) Elastic scattering (and hence greater path length in detector) of protons entering through the collimator.

(4) Inelastic nuclear interactions of protons in the detector and in other material of the satellite.

(5) Effects of electrons.

The importance of each process varies with position. Thus, processes (1) and (3) are more important in the outer zone than in

the inner zone, whereas processes (2), (4), and (5) are more important in the inner zone. We now consider each of these processes in detail.

(1) Proton pulse pile-up.

Whenever two protons, the sum of whose energies deposited in the detector exceeds 1.8 MeV, strike the detector within a sufficiently short time interval their pulses add up electronically so as to trigger the 1.8 MeV discrimination level (channel C) (Figure 2). Any such accidental double coincidences contribute ("spuriously") to the counting rate of C. Since channels A and B are both counting protons, we have a continuous knowledge of the intensity and the spectrum of protons in the radiation zones. Channel B counts protons in the interval $0.90 \leq E_p \leq 1.8$ MeV and we may use its counting rate to estimate the expected counting rate of C due to double coincidences.

Pulses from the detector are double-delay-line clipped and have a rectangular profile whose time width

$$\tau = 0.10 \ \mu s.$$

The rate of accidental double coincidences

$$R_2 = K_2 \tau R_1^2 , \qquad (1)$$

where R_1 is the rate of singles and K_2 is a factor which must be less than 2.0. In laboratory tests on a number of units

similar to that flown on Injun IV, including the flight back-up unit, equation (1) has been found to be accurately valid. Using both particles and a laboratory double-pulse generator the value of $K_2 \tau$ has been determined to lie between 0.08 and 0.12 μs. Hence, we take $K_2 = 1.0$, $\tau = 0.10$ μs and estimate R_2 in flight by the equation

$$R_2 = \tau R_1^2 . \qquad (2)$$

The highest value of R_2 is expected at the outer zone maximum of proton intensity (cf. Figure 4). It is already evident from the approximate constancy of the counting rate ratios A/C and B/C in the range $2.6 < L < 4.2$ (Figures 4 and 9) that the rate of C is <u>not</u> a quadratic function of the rate of either A or B. A quantitative estimate of R_2 is as follows.

At L = 3.05, $|\vec{B}|$ = 0.19

A = 800 counts/sec

B = 230

C = 0.2

Since the sum of two pulses large enough to trigger C must come from single pulses large enough to trigger B (Figure 2 and Table 1), we calculate the spurious rate of C to be

$$R_2 = \tau R_1^2 = (0.1 \times 10^{-6}) (230)^2$$
$$R_2 = 5 \times 10^{-3} \text{ counts/sec}$$

This is less by a factor of 40 than the observed rate of C.

The rate of accidental triple coincidences

$$R_3 = K_3 \tau^2 R_1^3 \qquad (3)$$

where K_3 is also of the order of unity. A high estimate of R_3 is obtained by supposing that all pulses large enough to trigger A can combine by threes to trigger C. Using equation (3), the estimated contribution of accidental triple coincidences to the rate of C is

$$R_3 = (0.1 \times 10^{-6})^2 (800)^3$$
$$R_3 = 5 \times 10^{-6} \text{ counts/sec,}$$

a value much less than R_2, and less than C by a factor of 2.5×10^{-5}.

A more rigorous estimate of R_2 can be made as follows. Channel B responds to protons in the energy range $0.90 \leq E_p \leq 1.8$ MeV and the maximum stopping power of the detector for protons is 1.3 MeV. The observed proton energy spectrum at the outer zone intensity maximum [Krimigis, 1967b] is

$$\frac{dj}{dE_p} = 1.4 \times 10^4 \exp(-E/0.30 \text{ MeV}) \text{ counts } (\text{sec MeV})^{-1} . \quad (4)$$

Using this spectrum and pairing protons over the entire energy range (i.e., 0.5 MeV with 1.3 MeV, 0.8 MeV with 1.0 MeV, etc., such that the sum of the pulse height is always greater than 1.8 MeV), we find

$$R_2 = 7.5 \times 10^{-3} \text{ counts/sec}$$

for the accidental double coincidence rate of C. Although somewhat larger than the simpler, more direct estimate given above, this rate is still less than the observed rate of C by a factor of 27.

Finally we note that the contribution of accidental coincidences to the rate of channel D is also negligible since triple coincidences of 1.3 MeV pulses (the largest possible from straightforward penetration of the detector) are necessary (and barely adequate) to produce counts in D.

We conclude that nowhere in either the outer or inner radiation zones can a significant fraction of the observed counting rates of either C or D be due to accidental coincidences of proton pulses.

(2) Transverse penetration of the detector by high energy protons.

The silicon detector is a thin, approximately circular disc of thickness 2.5×10^{-3} cm (5.83 mg/cm^2) and diameter 0.15 cm (350 mg/cm^2). The flat faces of the disc are perpendicular to the axis of the collimator. The ratio of the frontal to the projected lateral area is 47.

The design of the brass collimator is such that it provides essentially uniform shielding of 10.2 g cm^{-2} over about 8 steradians except within a conical core of half-angle 20° centered on its axis (Figure 1). Over the remainder of the solid angle the detector is more heavily shielded, both by local material and by the satellite itself. Thus, only protons whose original energy exceeds 95 MeV are able to reach the detector through the shield. Such protons are present only in the inner radiation zone and have an angular distribution which is sharply peaked at a pitch angle of 90° to $\vec{B}$. (A proton which traverses the detector along a diameter can lose a maximum of 15 MeV therein.) By virtue of the disc-like angular distribution, the contribution of penetrating protons is a maximum at $\varphi = 0°$ and 180° and is estimated to be less by a factor of 4 to 8 at $\varphi = 90°$. Figure 8 suggests the importance of an effect of this kind in the inner zone (in contrast to Figure 10 for the outer zone).

Figure 11 illustrates the geometric situation corresponding to the period of magnetic alignment of the satellite, $\varphi = 90°$.

The angular nomenclature of this figure will also be used for the case of $\varphi = 0°$ or 180°; in this case $\vec{B}$ is parallel to the detector axis and the "direction of maximum proton intensity" is parallel to the plane of the detector and rotationally symmetric. This latter situation is the one in which the maximum effect of penetrating protons is expected.

An estimate of the magnitude of the effect at $L \sim 1.5$ and for $\varphi = 0°$ proceeds along the following lines:

(a) Only protons having an original energy exceeding 95 MeV can reach the detector.

(b) After penetration of the shield, a proton must have a residual energy of at least 1.8 MeV (threshold of channel C) and must be moving at a sufficiently small angle to the plane of the detector so that its path through the detector permits it to deposit more than 1.8 MeV. The maximum value of this angle (α_C in Figure 11) is 35° for a proton having exactly 1.8 MeV in order that it trigger channel C. Protons striking the detector with energies > 1.8 MeV must be incident at appropriately smaller angles. The corresponding quantities for channel D are 3.7 MeV minimum residual energy and 10° maximum angle (α_D in Figure 11).

(c) For the region of interest in the inner zone ($L \sim 1.5$, $|\vec{B}| \sim 0.18$) we adopt a differential spectral intensity for the original beam

$$\frac{dj}{dE_p} = 1.0 \ (cm^2 \text{ sec sr MeV})^{-1}$$

in the vicinity of E_p = 100 MeV [Freden, 1966] and take it to be constant over the energy range which is pertinent to this calculation.

(d) The highest energy which need be considered is that of a proton which can just deposit 1.8 MeV (for C) or 3.7 MeV (for D) as it traverses the detector along a diameter--that is, whose specific ionization has fallen to 5.1 MeV cm^2/g (for C) or 10.6 MeV cm^2/g (for D). The corresponding values of residual energy are 120 or 45 MeV and the original values of energy E_{max} before striking the shield are 165 or 110 MeV [Janni, 1966].

(e) Since most of the protons in question have pitch angles within $\pm$ 20° of 90°, the available range of α in Figure 11 is not fully utilized.

(f) The projected geometric area of the detector at angle α is 0.0175 (sin α + 0.021 cos α). The effective area S (E,α) for any specified original energy E is a function of E as well as of α, being approximately equal to the above value for E ~ 100 MeV and zero for E = E_{max}.

(g) Thus, the counting rate of channel C (or D) due to transverse penetrations of the detector is given by:

$$R_T \approx \frac{dj}{dE} \int_{E_{min}}^{E_{max}} dE \int_{o}^{\alpha(E)} S(E,\alpha)\ (4\pi d\alpha)$$

$$R_T \approx (2\pi)\ (0.0175) \int_{E_{min}}^{E_{max}} \alpha^2\ (E)\ dE\ . \qquad (5)$$

Numerical estimates using (5) give

R_T for C $\approx$ 0.2 counts/sec

R_T for D $\approx$ 0.04 counts/sec .

These estimates, crude as they are, do show that the contributions of side-wall traversals by high energy protons are indeed of the same order of magnitude as the observed counting rates of C and D in the inner zone when $\varphi \sim 0°$ or 180° (Figure 8). (A similar estimate gives a plausible explanation for the $\varphi \sim 0°$ and 180° counting rates of Detectors A and B (cf. Figure 12).) Such "spurious" contributions decrease monotonically as φ goes toward 90° and are less by an estimated factor of 4 to 8 at $\varphi \sim 90°$.

The direct experimental evidence supports the belief that, even in the inner zone, channels C and D are measuring a true component of heavy nuclei during the magnetically aligned period. First, there is the counting rate peak at $\varphi = 90°$ in Figure 8. Secondly and more persuasively, there is a markedly different L-dependence of the rates of channel C (and D) and of the penetrating proton detector SpB (Table 1) as shown in Figure 13.

In the outer zone there is a virtually complete absence of penetrating protons and side-wall traversals are completely negligible there (see also Figure 10).

(3) Elastic scattering of protons entering through the collimator.

From the energy spectrum given by equation (4) one finds that there are ~ 1600 protons $(cm^2 \text{ sec sr})^{-1}$ with $E_p \gtrsim 1.8$ MeV perpendicular to $\vec{B}$ at the intensity maximum in the outer zone. On rare occasions one or these protons is deflected by elastic scattering in the detector or in the inner wall of the collimator in such a way that its total path in the detector is increased sufficiently to trigger channel C and, much more rarely, channel D. The probability of such scattering can be estimated by means of the Rutherford formula for protons:

$$dp = \pi\, n\, t \left(\frac{Z\, e^2}{M\, v^2} \right) \cot(\theta/2)\, \csc^2(\theta/2)\, d\theta \qquad (6)$$

where dp = probability of scattering into $d\theta$ at angle θ to the original direction

n = no. of nuclei per unit volume of the target

t = thickness of the target

Ze = charge of target nucleus

e = charge of incident particle

M = mass of incident particle

v = velocity of incident particle

The least scattering is required for particles entering the detector at the maximum angle (20°) to the axis of the detector. Specifically, a proton of 1.8 MeV must be deflected by 35° (versus 55° if incident axially) in order to lose its entire energy in the detector if the scattering occurs at the front face. Higher energy particles must be deflected by a greater angle in order to be counted. Also dp is inversely proportional to energy and is a steeply falling function of increasing θ. Only large angle, single scattering need be considered.

Hence, a clear upper limit P_{max} is obtained by supposing that all protons $E_p > 1.8$ MeV have $E_p = 1.8$ MeV, that all scattering throughout the detector occurs at the front face and that scattering is always away from the axis of the collimator. For simplicity the integration is extended to 180°, without affecting the result. Inserting the appropriate numbers for a 1.8 MeV proton and the constants for silicon into equation (6)

$$P_{max} = \int_{\theta=35°}^{180°} dp = 1.22 \times 10^{-4} \int_{35°}^{180°} \cot(\theta/2) \csc^2(\theta/2)\, d\theta$$

$$P_{max} = 1.2 \times 10^{-3} \quad . \qquad (7)$$

In a directional intensity of 1.6×10^{3} $(cm^{2}\ sec\ sr)^{-1}$ of protons $E_p > 1.8$ MeV, (1.6×10^{3}) $(6.4 \times 10^{-3}) = 10$ such particles enter the detector per second. Thus, an upper limit to the counting rate of channel C by Rutherford-scattered protons is

$$R_S = 1.2 \times 10^{-2} \text{ counts/sec.}$$

This rate (a generous upper limit) is less by a factor of 17 than the observed counting rate of 0.2 counts/sec. Moreover, the experimentally measured value of the proton efficiency (i.e., a value for P) for channel C was found to be less than 3×10^{-4} for axially-incident protons $E_p = 1.8$, 1.9, 2.05, and 3.57 MeV. (Section 2)

We conclude that elastically scattered protons $E_p \geq 1.8$ MeV (as well as unscattered ones of any energy) make a negligible contribution to the counting rate of channels C and D.

(4) Inelastic nuclear interactions of protons in the detector and in other material of the satellite.

In addition to elastic scattering, one must consider inelastic nuclear interactions. There are several reactions of possible importance involving Si^{28} [Endt and Van der Leun, 1962]: viz., Si^{28} (p,p') Si^{28}, Si^{28} (n,p) Al^{28}, and Si^{28} (n,α) Mg^{25}. Each of these reactions has to be evaluated on the basis of its cross-section and the probability that the outgoing particle may

deposit enough of its energy in the detector to be counted in channel C. The reaction Si^{28} (p,p') Si^{28} can contribute to the counting rate if the proton is emitted in such a direction that it deposits at least 1.8 MeV in the detector. Typical cross-sections for this reaction are ~ 165 millibarns (mb) at $E_p \simeq 12$ MeV [Conzett, 1957] and ~ 30 mb/sr at $4.8 < E_p <$ MeV [Yamabe et al., 1958]. Assuming that (a) the average cross section is ~ 100 mb and (b) all inelastically scattered protons with $E_p \gtrsim 1.8$ MeV are counted in C, and using the known intensity of such protons, one finds that the contribution to the rate of channel C is ~ 8×10^{-5} counts/sec. This rate is ~ 10^4 times smaller than the observed rate of C.

Trapped protons incident on the skin of the satellite produce neutrons in various nuclear reactions and the resulting neutrons can [R. R. Carlson, private communication] interact with silicon in the reactions Si^{28} (n,p) Al^{28} and Si^{28} (n,α) Mg^{25}. The cross sections for both of these reactions are as great as 400 mb at neutron energies of ~ 8 MeV, decreasing to essentially zero at ~ 5 MeV and at ~ 20 MeV [Stehn et al., 1964]. From the known intensities of trapped protons in the region of interest and the size and constitution of the satellite, we estimate that the resulting counting rate of channel C from (n,p) and (n,α) reactions is $\lesssim 10^{-6}$ counts/sec.

Experimental evidence for the neglect of any such effects is as follows: (a) During the calibration runs at NRL described in part 2, the proton beam of several microamperes was stopped in the brass chamber containing the detector and a large number of neutrons was generated (the reaction threshold for protons on Cu^{65} is 2.165 MeV and proton energies of up to 3.57 MeV were used), but no counts attributable to neutrons were observed. (b) The flight spare unit was exposed to a flux of $\sim 8 \times 10^3$ neutrons $(cm^2\ sec)^{-1}$ from the University of Iowa Van de Graaff accelerator and only one count was observed in $\sim$ 2 hours. Hence the observed efficiency must be $\lesssim 10^{-6}$.

In addition to the above reactions one might consider nuclear star production due to high energy (tens of MeV) protons. The cross section for such processes is small and there is direct experimental evidence that they could not be a significant source of counts for channel C. The evidence is shown in Figure 13, where the counting rates of detector SpB (sensitive to protons of $E_p \gtrsim 70$ MeV) and channel C have been plotted as a function of L. It is observed that there is marked dissimilarity between these two curves. Moreover, Figure 10 provides direct evidence against the importance of any type of nuclear interactions in the body of the satellite in the outer zone.

(5) Effects of electrons.

The small physical size of the detector and the 0.10 μs pulse clipping serve to make it exceedingly insensitive to electrons of any energy. Moreover, the discrimination levels of channels C and D (1.8 and 3.7 MeV) are far above the energies of most geomagnetically trapped electrons (except for the residuum of β-decay electrons from the Starfish nuclear burst of 9 July 1962 in the inner zone). For example, the thickness of the detector corresponds to the extrapolated range of only a 60 keV electron or to a mean energy loss of about 15 keV for a fast electron. The diameter corresponds to the extrapolated range of a 900 keV electron.

By pre-flight laboratory tests with 2 MeV electrons from a magnetic spectrometer (courtesy L. A. Frank) and by the flight data from a similar detector on Mariner IV [Krimigis and Armstrong, 1966] it has been established that effects of electrons on the counting rates of any one of the channels A, B, C, or D are negligible throughout the magnetosphere. There are also direct Injun IV data on the intensity of electrons $E_e \gtrsim 1.6$ MeV (from another detector) which have a completely different L dependence than do the data from channels C and D (in a manner quite similar to the comparison given in Figure 13).

6. INTERPRETATION OF COUNTING RATES OF CHANNELS C AND D

On the strength of the data and discussion of sections 2, 3, 4, and 5, we conclude that the counting rates of channels C and D during the magnetically aligned period are due almost exclusively to the direct detection of geomagnetically trapped nuclei having $Z \geq 2$. Neither He^3 nor nuclei heavier than He^4 can be excluded but on the basis of their low relative abundances in the earth's atmosphere, in the sun's atmosphere, and presumably in the solar wind, we will henceforth regard the responses of channels C and D as due solely to geomagnetically trapped alpha particles.

7. SPECTRA AND RELATIVE INTENSITIES OF PROTONS AND ALPHA PARTICLES IN THE OUTER ZONE

In the spirit of the remarks in section 1, it is desirable to have a full knowledge of the respective absolute spectra and angular distributions of protons and alpha particles throughout the magnetosphere. The present investigation provides a modest beginning.

It is noted that the energy "pass bands" of our channels A and C were chosen in such a way that both their lower and upper energy limits (Table 1) if expressed in kinetic energy/nucleon ($\mathcal{E}$) are identical for protons and alpha particles, respectively:

Channel A: $0.52 \leq \mathcal{E}_p \leq 4$ MeV/nucleon

Channel C: $0.52 \leq \mathcal{E}_\alpha \leq 4$ MeV/nucleon

The geometric factor of the detector is identical, of course, for all four channels. Hence, the ratio of counting rates in channels C and A (after subtraction of the background due to the in-flight calibrating source) provides a direct and unequivocal intensity ratio j_α/j_p integrated over the common range of $\mathcal{E}$ noted above. This ratio characterizes a common range of particle velocity and is independent of any assumptions regarding spectral forms. (Further, if the angular distributions of the two species of particle are identical and if the respective spectra

are independent of pitch angle, the j_α/j_p ratio is also the ratio of number densities in the specified velocity range. Neither of these latter conditions is known to be fulfilled, however.)

The most accurate and reliable value of the direct ratio described above is obtained at the outer zone intensity maximum $L \approx 3.1$, at the lowest value of $|\vec{B}|$ (0.19 gauss) for which adequate observations are available, and for $\varphi = 90°$ (Figure 9). This value is:

$$j_\alpha/j_p = (2.3 \pm 0.2) \times 10^{-4},$$
$$0.52 \leq \mathcal{E}_\alpha, \mathcal{E}_p \leq 4 \quad \text{MeV/nucleon.} \qquad (8)$$

The latitude parameter $|\vec{B}| / |\vec{B}_o| = 18$. By virtue of the rapid decline of both $dj/d\mathcal{E}_\alpha$ and $dj/d\mathcal{E}_p$ with increasing $\mathcal{E}$, the ratio given in (8) is accurately equal to the more simple ratio:

$$j_\alpha/j_p = (2.3 \pm 0.2) \times 10^{-4},$$
$$\mathcal{E}_\alpha, \mathcal{E}_p \geq 0.52 \text{ MeV/nucleon.} \qquad (9)$$

We regard this value as the most important and trustworthy result of the present investigation.

Since the detector has two proton channels (A and B) and two alpha particle channels (C and D), spectral information of an approximate nature can also be derived. In the absence of significant theoretical guidance, we have fit two-point spectra

to six different, simple spectral forms--both exponentials and power laws in kinetic energy, in kinetic energy/nucleon, and in magnetic rigidity. The results of this work are summarized in Table 2 for $2.8 \leq L \leq 3.3$ and $|\vec{B}| = 0.19 \pm 0.01$ gauss. It is clear that the implications of the various spectral assumptions are strikingly different. For example, in Figure 14 we show the expected ratio of the integrated intensities j_α/j_p above the kinetic energy or kinetic energy/nucleon labeled on the scale of abscissa for two different exponential spectra from Table 2.

The value of $(dj_\alpha/dE_\alpha)/(dj_p/dE_p) \approx 0.05$ at $E_\alpha = E_p = 2$ MeV in our original report [Van Allen and Krimigis, 1965] was derived from assumed exponential spectra in kinetic energy. Although the raw observational data available at that time (though less complete) were similar to those reported herein, it is clear from Table 2 and Figure 14 that the originally reported spectral ratio should be regarded as an inadequate and perhaps misleading representation of the overall situation.

From inspection of Figure 14 and Table 2, it is difficult to avoid the impression that j_α/j_p is an increasing (and perhaps a strongly increasing) function of increasing energy or energy/nucleon or magnetic rigidity and this result may be one of validity and of physical significance.

In view of the fact that the proton spectrum in the outer zone is best represented by an exponential in energy [Davis and Williamson, 1963; Hoffman and Bracken, 1965; Armstrong and Krimigis, 1967], there is a certain intuitive preference for expressing the alpha particle spectrum as an exponential in energy/nucleon. When this is done the integral j_α/j_p ratio is not a strong function of $\mathcal{E}$ and might even be independent of $\mathcal{E}$. (See the uncertainty stripe in Figure 14.)

8. SPECTRA AND RELATIVE INTENSITIES OF PROTONS AND ALPHA PARTICLES IN THE INNER ZONE

In the inner zone, $1.8 < L < 2.2$, $|\vec{B}| = 0.19 \pm 0.01$ gauss,

$$j_\alpha / j_p = 1.1 \times 10^{-3},$$
$$\mathcal{E}_\alpha, \mathcal{E}_p \geq 0.52 \text{ MeV/nucleon} \qquad (10)$$

and the spectra of protons and alpha particles are given by

$$\frac{dj_p}{d\mathcal{E}} = 7.7 \times 10^4 \exp(-\mathcal{E}/0.37) \qquad (11)$$

and

$$\frac{dj_\alpha}{d\mathcal{E}} = 68 \exp(-\mathcal{E}/0.41) . \qquad (12)$$

The same units are used in equations (11) and (12) as in Table 2.

9. DISCUSSION

The most widely accepted conjecture for the origin of energetic particles in the outer zone is that they have been injected from the solar wind into trapped orbits in the magnetosphere and subsequently accelerated and diffused across magnetic shells therein by complex electromagnetic processes.

The ratio of the number densities of alpha particles and protons in the solar wind is 0.01 to 0.1 [Neugebauer and Snyder, 1966; Coon, 1965; Wolfe et al., 1966; Gosling et al., 1967].

Tverskoy [1965] and Hess [1966] have given some consideration to the relative spectral treatment of alpha particles and protons in the framework of the solar-wind-source model. On the assumption that both protons and alpha particles are "thermalized" to the same kinetic energy in the transition region, Hess finds that the spectrum of alpha particles would also be of exponential form in particle energy (since the proton spectrum is known observationally to be of this form) and that the two spectra would have identical values of e-folding energy per particle (not energy per nucleon) at a given L value for $L \gtrsim 3$. He also predicts that the ratio of spectral intensities will be of the same order as that of the number densities in the solar wind (i.e., ~ 0.05). Our results at $L \simeq 3.1$ appears to be in clear disagreement with both of these

expectations (Table 2 and Figure 14), though we should note that our measurements are made in a region far from the equator ($|\vec{B}| / |\vec{B}_o| = 18$). This latter fact may invalidate the comparison, as noted by Hess, since he has assumed the absence of energy losses in his preliminary work. Such an assumption is clearly less valid for particles having mirror points at low altitudes than for those having mirror points near the equator. There are indications, however, that at this value of $|\vec{B}| / |\vec{B}_o|$ the effect of the atmosphere may not be important [Krimigis, 1967b].

On the other hand, our results are not strongly inconsistent with a ratio $(dj_\alpha/d\mathcal{E}_\alpha)/(dj_p/d\mathcal{E}_p)$ which is independent of energy per nucleon (i.e., of velocity) (lower curve Fig. 14). This suggests, following Tverskoy, that protons and alpha particles may be "thermalized" to the same velocity rather than to the same energy and that in the trans-L diffusion process the same spectral form is maintained in terms of energy/nucleon. A further consideration is the Coulomb energy loss of particles traversing the outer atmosphere. Thus

$$-\frac{dE}{dx} \propto \frac{Z^2}{v^2} \qquad (13)$$

is the rate of energy loss per unit path length x in the atmosphere for a non-relativistic particle having charge Z and velocity v. Substituting dx = vdt in (10) and integrating,

$$t \propto \frac{E^{3/2}}{Z^2 M^{1/2}} \qquad (14)$$

where M is the mass of the particle. Hence, for protons and alpha particles of the same initial energy, their lifetimes against Coulomb energy loss are related by the equation:

$$t_p = 8\, t_\alpha \qquad (15)$$

if the particles remain fully ionized throughout their range. The actual factor is somewhat less than 8 for the energies under consideration here. For particles having the same initial velocity, however:

$$t \propto \frac{Mv^3}{Z^2} \qquad (16)$$

and thus

$$t_p = t_\alpha \,. \qquad (17)$$

These considerations illustrate Tverskoy's suggestion that spectra in terms of energy/nucleon may be more appropriate whenever Coulomb energy losses in the atmosphere are important. Another loss process which may influence proton and alpha particle spectra in a different way is charge exchange in the atmosphere. No treatment of this subject for alpha particles is known to us.

Tverskoy [1965] makes the following specific predictions: (a) The intensity maximum for 2 MeV α-particles should be located at $L \simeq 3.2$, and this intensity should be $\sim 10^3$ $(cm^2\ sec)^{-1}$ at the equator. (b) The j_α/j_p ratio at that point for particles with total energy greater than 2 MeV should be $\sim 10^{-3}$. Comparing with Figure 3 we find that the location of the maximum as well as the

flux are approximately correct, if one takes into account the magnetic coordinates of the observations and assumes that the α-particles are evenly distributed over $\sim 2\pi$ steradians. Regarding his point (b) we find from Figure 14 that Tverskoy's ratio is smaller from that observed by an order of magnitude although, at a lower energy ($\sim$ 700 keV), his prediction would have been correct. We note that Tverskoy and Hess have a certain level of agreement in that Hess predicts a ratio of 0.05 which is independent of energy and does not include any losses and Tverskoy predicts a ratio of 10^{-3} which is also independent of energy but includes Coulomb losses. The factor of ten difference is due to the Coulomb losses alone.

From the foregoing, it appears conceivable that the observed ratio j_α/j_p may be reconcilable with a solar-wind-source of outer zone protons and alpha particles, although this ratio is significantly less than that predicted from diffusion theory with known loss processes taken into account.

However, the exosphere of the earth also contains a mixture of hydrogen and helium and it is not yet obvious that in situ acceleration processes could not yield the observed situation, with atmospheric ions as the source particles.

The j_α/j_p ratio appears to be larger in the inner zone (Section 8) than in the outer zone. Also the L dependence of j_α (Figures 3, 4, 5, and 6) suggests that the source of inner zone

alpha particles may be altogether different than the source of outer zone alpha particles. It is pointed out, however, that equation (10) represents an average value over the L range 1.8-2.2 where the proton intensity changes by a factor of 4 (Figure 4). Thus, although this value is significantly different than that in the outer zone, it does not lend itself to the type of analysis presented in the previous section. Specific sources of inner zone alpha-particles, which we have not assessed quantitatively, are proton-induced nuclear stars in the atmosphere and radioactive-decay of miscellaneous fission products [G. F. Pieper, private communication] from several high altitude nuclear bursts which have occurred in this region.

10. REMARKS ON TIME VARIATIONS

The data described so far were taken during the period before 17 April 1965. On April 17 a geomagnetic sudden commencement occurred at ~ 1312 UT and was followed by a magnetic storm with a main phase depression of the horizontal field of ~ 160 γ. The distribution of 0.5 MeV protons measured by Injun IV was severely and durably disturbed [Krimigis, 1967a]. The distribution of alpha particles for the period 17 April--31 May in Figure 15 and the previously discussed 1 March--17 April distribution has been included for comparison. It is observed that the maximum intensity increased by ~ 30% and the position of the maximum moved inward to $L \simeq 2.9$. We expect that the subsequent time history of the distribution of alpha particles and its relationship to that of protons will provide some additional insight on the dynamics of both components. Such a study is underway.

11. CONCLUSIONS

(a) The presence of geomagnetically trapped alpha particles is established.

(b) At constant $\left| \vec{B} \right| \approx 0.19$ gauss the maximum intensity perpendicular to $\vec{B}$ occurs at L = 3.1. The absolute directional intensity there is

$$j_\alpha (E_\alpha > 2.09 \text{ MeV}) = 28 \text{ (cm}^2 \text{ sec sr)}^{-1} \text{ and}$$
$$j_\alpha (E_\alpha > 3.89 \text{ MeV}) = 4.5 \text{ (cm}^2 \text{ sec sr)}^{-1} .$$

(c) At this outer zone maximum, the ratio of the directional intensities of alpha particles and of protons, both integrated above the common value $\mathcal{E}_\alpha = \mathcal{E}_p = 0.52$ MeV/nucleon, is

$$j_\alpha / j_p = (2.3 \pm 0.2) \times 10^{-4} .$$

(d) A variety of considerations, no one of which is decisive, suggest that the most physically significant form of the spectra of alpha particles and protons may be an exponential one in terms of energy/nucleon.

(e) It appears conceivable that the observed ratio j_α / j_p may be reconcilable with a solar-wind-source of outer zone protons and alpha particles although this ratio is significantly less than that predicted from diffusion theory with known loss processes taken into account.

(f) The distribution of outer zone alpha particles was changed markedly after the magnetic storm of 18 April 1965 and the intensity peak moving inward from L = 3.1 to L = 2.9.

(g) Trapped alpha particles in the inner zone are apparently due to a different source than that for those in the outer zone.

12. ACKNOWLEDGEMENTS

We thank Dr. T. P. Armstrong for experimental assistance and useful discussions regarding the results. Messrs. W. A. Whelpley, F. Zamecnik, J. C. Craven, and K. L. Ackerson have been responsible for the organization and conduct of the Injun IV data reduction. Mr. E. Wolicki of the Naval Research Laboratory kindly made facilities available for the calibration of the detector. Messrs. D. Enemark, E. Strein, B. Randall, W. Greene, and R. Ganfield contributed to the electronic design and experiment testing and assisted with proton calibrations at the University of Iowa. Messrs. A. L. Burns, C. M. Tsai, and J. Bakas assisted with the data reduction while L. Shope, B. Brechwald, and P. Dalamaggas were responsible for most of the programming effort. H. Kiel supervised the execution of the programs. We thank Mr. W. A. Whelpley of the University of Iowa and C. W. Coffee of Langley Research Center, as well as many University of Iowa and LRC personnel, too numerous to mention by name, who contributed to making the Injun IV satellite a success.

Development, construction, and preflight testing of the University of Iowa satellite Injun IV was performed under contract NAS1-2973 with the National Aeronautics and Space Administration/

Langley Research Center. Analysis and publication have been performed in part under National Aeronautics and Space Administration grant NsG 233-62 and the Office of Naval Research Contract Nonr 1509(06).

Table 1

Characteristics of the Injun IV Detectors

Detector	Unidirectional Geometric Factor cm^2 steradian	Omnidirectional Geometric Factor cm^2	Particles to Which Sensitive		Dynamic Range
A	0.0064 ± 0.0007	---	Protons:	$0.52 \leq E_p \leq 4$ * MeV	From inflight source to 10^6 c/sec
			Electrons:	None	
B	0.0064 ± 0.0007	---	Protons:	$0.90 \leq E_p \leq 1.8$* MeV	"
			Electrons:	None	
C	0.0064 ± 0.0007	---	α-Particles:	$2.09 \leq E_\alpha \leq 15$* MeV	"
			Tritons:	See Text	
D	0.0064 ± 0.0007	---	α-Particles:	$3.89 \leq E_\alpha \leq 7$ * MeV	"
SpB	---	~ 0.4	Protons:	$E_p \gtrsim 70$ MeV	From galactic cosmic ray rate of 2 c/s to 2×10^5 c/sec
			Electrons:	Insensitive except via bremsstrahlung for $E_e \gtrsim 1$ MeV	

*Upper limit for axial incidence; the corresponding limits for incidence at 20° to the collimator axis are 4.2, 1.9, 18, and 8 MeV for A, B, C, and D, respectively.

**A, B, C, and D correspond to different electronic discrimination levels in the same basic detector.

Table 2

Various Two Point Proton and Alpha Particle Spectra in the Proton Zone
($L = 2.8$ to 3.3, $|\vec{B}| = 0.19 \pm 0.01$ gauss)

Spectral Parameter and Range	Power Law	j_α/j_p	Exponential Law	j_α/j_p
E, Total Energy $E \geq 0.52$ MeV	$\frac{dj_p}{dE} = 62{,}700\ E^{-3}$	1.5×10^{-3}	$\frac{dj_p}{dE} = 2.16 \times 10^{6} \exp(-E/0.30)$	6.3×10^{-4}
	$\frac{dj_\alpha}{dE} = 95.8\ E^{-2.32}$		$\frac{dj_\alpha}{dE} = 68.8 \exp(-E/1.50)$	
$\mathcal{E}$, Energy per Nucleon $\mathcal{E} \geq 0.52$ MeV/nucleon	$\frac{dj_p}{d\mathcal{E}} = 62{,}700\ \mathcal{E}^{-3}$	2.3×10^{-4}	$\frac{dj_p}{d\mathcal{E}} = 2.16 \times 10^{6} \exp(-\mathcal{E}/0.30)$	2.2×10^{-4}
	$\frac{dj_\alpha}{d\mathcal{E}} = 15.4\ \mathcal{E}^{-2.35}$		$\frac{dj_\alpha}{d\mathcal{E}} = 280 \exp(-\mathcal{E}/0.37)$	
P, Magnetic Rigidity $P \geq 31.1$ MV	$\frac{dj_p}{dP} = 4.44 \times 10^{11}\ P^{-5}$	1.4×10^{-3}	$\frac{dj_p}{dP} = 6.62 \times 10^{-5} \exp(-P/8.1)$	9.5×10^{-4}
	$\frac{dj_\alpha}{dP} = 3.67 \times 10^{6}\ P^{-3.63}$		$\frac{dj_\alpha}{dP} = 21.4 \exp(-P/21.6)$	

Notes: (1) dj/dE has the units $(cm^2\ sec\ sr\ MeV)^{-1}$.

(2) dj/dP has the units $(cm^2\ sec\ sr\ MV)^{-1}$.

(3) $dj/d\mathcal{E}$ has the units $(cm^2\ sec\ sr\ MeV/nucleon)^{-1}$.

(4) The stated j_α/j_p ratios are of intensities integrated from the specified lower value of the spectral parameter in each case (E, $\mathcal{E}$, or P) to infinity.

REFERENCES

Armstrong, A. H., F. B. Harrison, H. H. Heckman, and L. Rosen, Charged Particles in the Inner Van Allen Radiation Belt, J. Geophys. Res., 66, 351-357, 1961.

Armstrong, T. P., and S. M. Krimigis, Observations of Protons in the Magnetosphere and Magnetotail with Explorer 33, J. Geophys. Res. (to be published), 1967.

Bates, D. R., and R. McCarroll, Charge Transfer, Advances in Physics, 11, 39-81, 1962.

Conzett, Homer E., Inelastic Scattering of 12-MeV Protons on Lithium, Carbon, Magnesium, and Silicon, Phys. Rev., 105, 1324, 1957.

Coon, J. H., Vela Satellite Measurements of Particles in the Solar Wind and the Distant Geomagnetosphere, pp. 231-255 of Radiation Trapped in the Earth's Magnetic Field, R. Reidel Publishing Co., Dordrecht-Holland, 1966 (ed. by B. M. McCormac).

Davis, L. R., and J. M. Williamson, Low-Energy Trapped Protons, Space Res., 3, 365-375, 1963.

Endt, P. M., and C. Van der Leun, Nucl. Phys., 34, 122-125, 1962.

Fenton, K. B., A Search for α-Particles in the Geomagnetic Field, Preprint No. EFINS 67-7, Laboratory for Astrophysics and Space Research, University of Chicago, 1967.

Fillius, R. W., Trapped Protons in the Inner Radiation Belt, J. Geophys. Res., 71, 97-123, 1966.

Freden, S. C., Energy Spectrum of Inner Zone Protons, pp. 116-128 of Radiation Trapped in the Earth's Magnetic Field, R. Reidel Publishing Co., Dordrecht-Holland, 1966 (ed. by B. M. McCormac).

Freden, S. C., J. B. Blake, and G. A. Paulikas, Spatial Variations of the Inner Zone Trapped Proton Spectrum, J. Geophys. Res., 70, 3113-3116, 1965.

Freden, S. C., and R. Stephen White, Particle Fluxes in the Inner Radiation Belt, J. Geophys. Res., 65, 1377-1383, 1960.

Freden, S. C., and R. Stephen White, Trapped Proton and Cosmic-Ray Albedo Neutron Fluxes, J. Geophys. Res., 67, 25-29, 1962.

Gosling, J. T., J. R. Asbridge, S. J. Bame, A. J. Hundhausen, and I. B. Strong, Measurements of the Interplanetary Solar Wind during the Large Geomagnetic Storm of April 17-18, 1965, J. Geophys. Res., 72, 1813-1821, 1967.

Hearendel, G., Protonen in Inneren Strahlungsgurtel, Fortschr. Physik, 12, 271-346, 1964.

Heckman, H. H., and A. H. Armstrong, Energy Spectrum of Geomagnetically Trapped Protons, J. Geophys. Res., 67, 1255-1262, 1962.

Hess, W. N., Source of Outer Zone Protons, pp. 352-368 of Radiation Trapped in the Earth's Magnetic Field, R. Reidel Publishing Co., Dordrecht-Holland, 1966 (ed. by B. M. McCormac).

Hoffman, R. A., and P. A. Bracken, Magnetic Effects of the Quiet-Time Proton Belt, J. Geophys. Res., 70, 3541-3556, 1965.

Imhof, W. L., and R. V. Smith, Proton Intensities and Energy Spectrums in the Inner Van Allen Belt, J. Geophys. Res., 69, 91-100, 1964.

Janni, J. F., Calculations of Energy Loss, Range, Path Length, Straggling, Multiple Scattering and the Probability of Inelastic Nuclear Collisions for 0.1 to 1000 MeV Protons, AFWL-TR-65-150 of Air Force Weapons Laboratory, Kirtland Air Force Base, New Mexico, 1966.

Kellogg, P. J., Van Allen Radiation of Solar Origin, Nature, 183, 1295, 1959.

Krimigis, S. M., Bifurcation of the Outer Zone 0.5 MeV Proton Distribution Following the April 18, 1965 Magnetic Storm, Trans. Am. Geophys. Union, 48, 163, 1967a [Abstract].

Krimgis, S. M., Observations of Low Energy (~ 0.5 MeV) Trapped Protons with Injun IV , presented at the Advanced Study Institute, "Earth's Particles and Fields", Freising, Germany, July 31--August 11, 1967b.

Krimigis, S. M., and T. P. Armstrong, Observations of Protons in the Magnetosphere with Mariner 4, J. Geophys. Res., 71, 4641-4650, 1966.

Krimigis, S. M., and J. A. Van Allen, Trapped Alpha Particles in the Earth's Radiation Zones, The Inter-Union Symposium on Solar Terrestrial Physics, Belgrade, August 29--September 2, 1966 [Post-Deadline Abstract].

Krimigis, S. M., J. A. Van Allen, and T. P. Armstrong, Trapped Alpha Particles in the Earth's Radiation Zones, Trans. Am. Geophys. Union, 48, 164, 1967 [Abstract].

Nakada, M. P., J. W. Dungey, and W. N. Hess, On the Origin of Outer-Belt Protons, J. Geophys. Res., 70, 3529-3532, 1965.

Nakada, M. P., and G. D. Mead, Diffusion of Protons in the Outer Radiation Belt, J. Geophys. Res., 70, 4777-4791, 1965.

Naugle, J. E., and D. A. Kniffen, Variations of the Proton Energy Spectrum with Position in the Inner Van Allen Belt, J. Geophys. Res., 68, 4065-4078, 1963.

Neugebauer, M., and C. W. Snyder, Mariner 2 Measurements of the Solar Wind, pp. 3-23 of The Solar Wind, Pergamon Press, 1966 (ed. by R. J. Mackin, Jr. and M. Neugebauer).

Stehn, J. R., M. D. Goldberg, B. A. Magurno, and R. Wiener-Chasman, Neutron Cross Sections, 1, Z = 1 to 20, Suppl. No. 2, BNL 325, 1964.

Tverskoy, B. A., Transport and Acceleration of Charged Particles in the Earth's Magnetosphere, Geomagnetism and Aeronomy, V, 617-628, 1965.

Valerio, J., Protons from 40 to 110 MeV Observed on Injun 3, J. Geophys. Res., 69, 4949-4958, 1964.

Van Allen, J. A., and S. M. Krimigis, Trapped Alpha Particles in the Earth's Outer Radiation Zone, Trans. Am. Geophys. Union, 46, 140, 1965 [Abstract].

Wolfe, J. H., R. W. Silva, D. D. McKibbin, and R. H. Mason, The Compositional, Anisotropic, and Nonradial Flow Characteristics of the Solar Wind, J. Geophys. Res., 71, 3329-3335, 1966.

Yamabe, Shotaro, Michiya Kondo, Takashi Yamazaki, and Atsutomo Toi, Angular Distribution of Protons Inelastically Scattered from Si^{28} and Mg^{24}, J. Phys. Soc. Japan, 13, 777-781, 1958.

FIGURE CAPTIONS

Figure 1. An assembly drawing showing the geometry of the Injun IV solid state detector collimator. Notice that particles penetrating the shield travel approximately the same path length at all angles of incidence within the outer hemisphere.

Figure 2. ΔE vs E curves for protons and α-particles incident on a 25 micron silicon detector with a 0.21 mg cm^{-2} nickel foil in front.

Figure 3. The L dependence of counting rates of channels C and D at constant $|\vec{B}|$ and at $\varphi = 90°$.

Figure 4. The L dependence of counting rates of channels A and C at constant $|\vec{B}|$ and at $\varphi = 90°$.

Figure 5. Contours of constant apparent intensity in $|\vec{B}|$ - L space. The labeled values on the several curves are the quotients of the counting rates of channel C by its geometric factor 0.0064 cm^2 sterad. Some of the counts may be due to other causes than direct entry of heavy nuclei through the collimator. There appear to be two different regimes, divided by the line L = 2.6.

Figure 6. Similar to Figure 5, but for channel D.

Figure 7. The dependence of the counting rates of channels A, B, C, and D on $|\vec{B}|$ in the inner zone.

Figure 8. The counting rate of channel C in the inner zone as a function of the angle φ between the collimator axis and the $|\vec{B}|$ vector.

Figure 9. Same as Figure 7 but for the outer zone.

Figure 10. Same as Figure 8 but for the outer zone. Note that there were no counts between 0° and 30° although these angles were sampled repeatedly.

Figure 11. Schematic representation of the geometry used in the calculation of R_T, section 5, paragraph 2, of the text (q.v.).

Figure 12. The counting rates of channels A and C in the inner zone as a function of φ. Note that the apparent contribution to the counting rate of A due by transverse penetrating particles is ~ 10 times that of C.

Figure 13. An illustration of the lack of dependence of the counting rate of C as $\varphi = 90°$ on the intensity of high energy protons.

Figure 14. Dependences of the ratio j_α/j_p of intensities of alpha particles and protons both integrated from the same lower limit specified by the abscissa to infinity. Both E (upper curve and top scale) and $\mathcal{E}$ (lower curve and bottom scale) have a common numerical scale of abscissa. The two curves are derived from Table 2. The cross hatched region indicates the region of uncertainty due to uncertainties in spectral fits.

Figure 15. The distribution of trapped α-particles before (solid line) and after (dashed line) the 17 April 1965 magnetic storm.

INJUN IV SOLID STATE DETECTOR APERTURE

G67-572

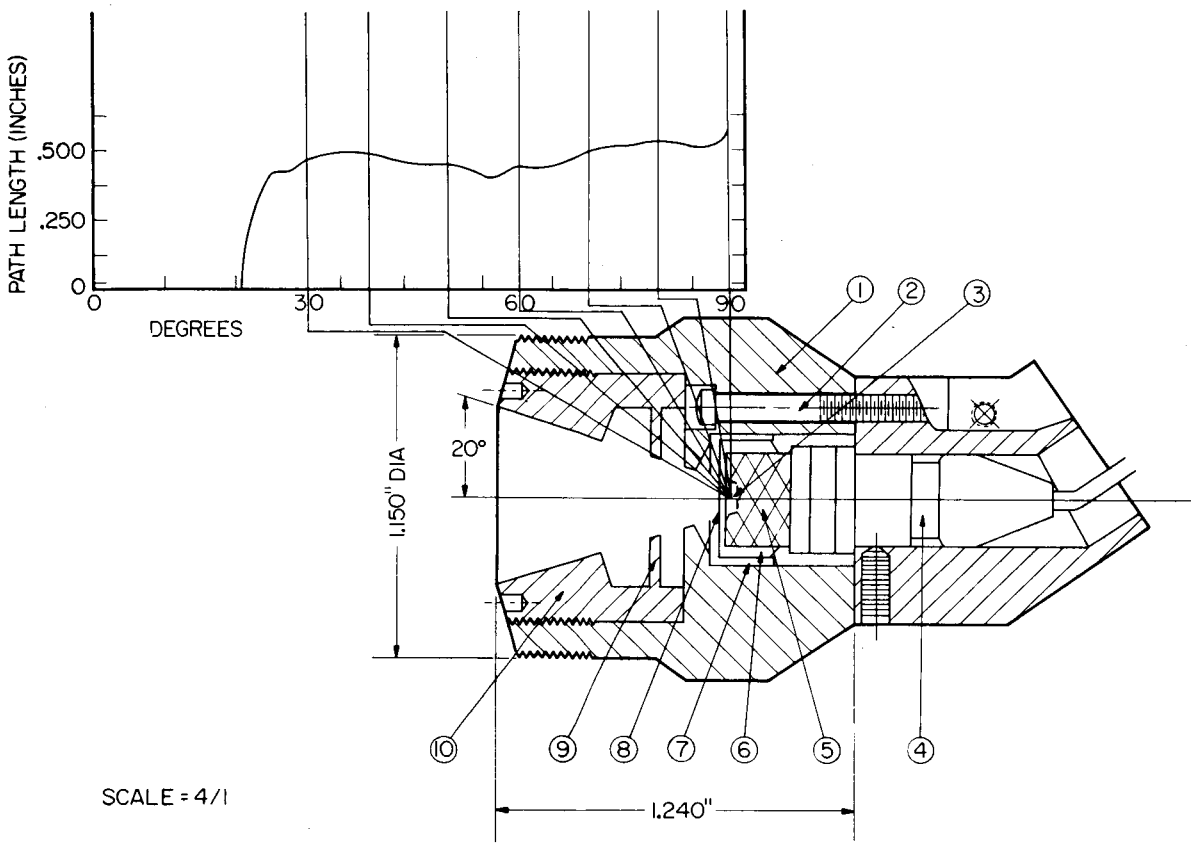

NO.	DESCRIPTION	MATERIAL
1	MAIN HOUSING	BRASS
2	MOUNTING SCREW	STAINLESS STEEL
3	NUCLEAR DIODE SURFACE BARRIER, TOTALLY DEPLETED DETECTOR	
4	MICRODOT CABLE	
5	MICRODOT DETECTOR MOUNT	
6	INNER FOIL HOLDER	SILVER-NICKEL
7	OUTER FOIL HOLDER	ALLOY
8	LIGHT-TIGHT FOIL	NICKEL
9	ELECTRON BAFFLE	BRASS
10	APERTURE DEFINING RING	BRASS

Figure 1

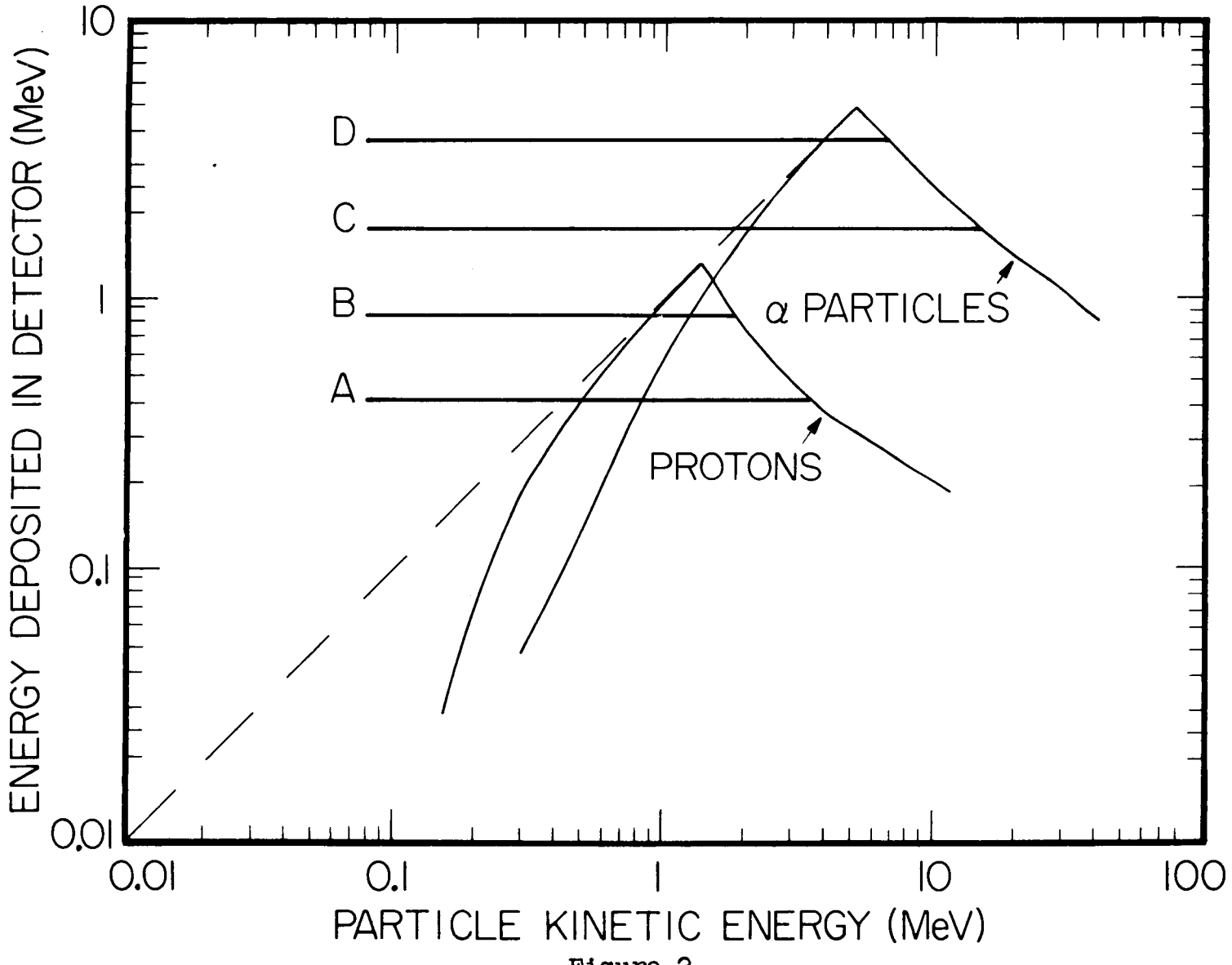
ENERGY DEPOSITED IN DETECTOR (MeV)
10
1
0.1
0.01
D
C
B
A
α PARTICLES
PROTONS
0.01
0.1
1
10
100
PARTICLE KINETIC ENERGY (MeV)

Figure 2

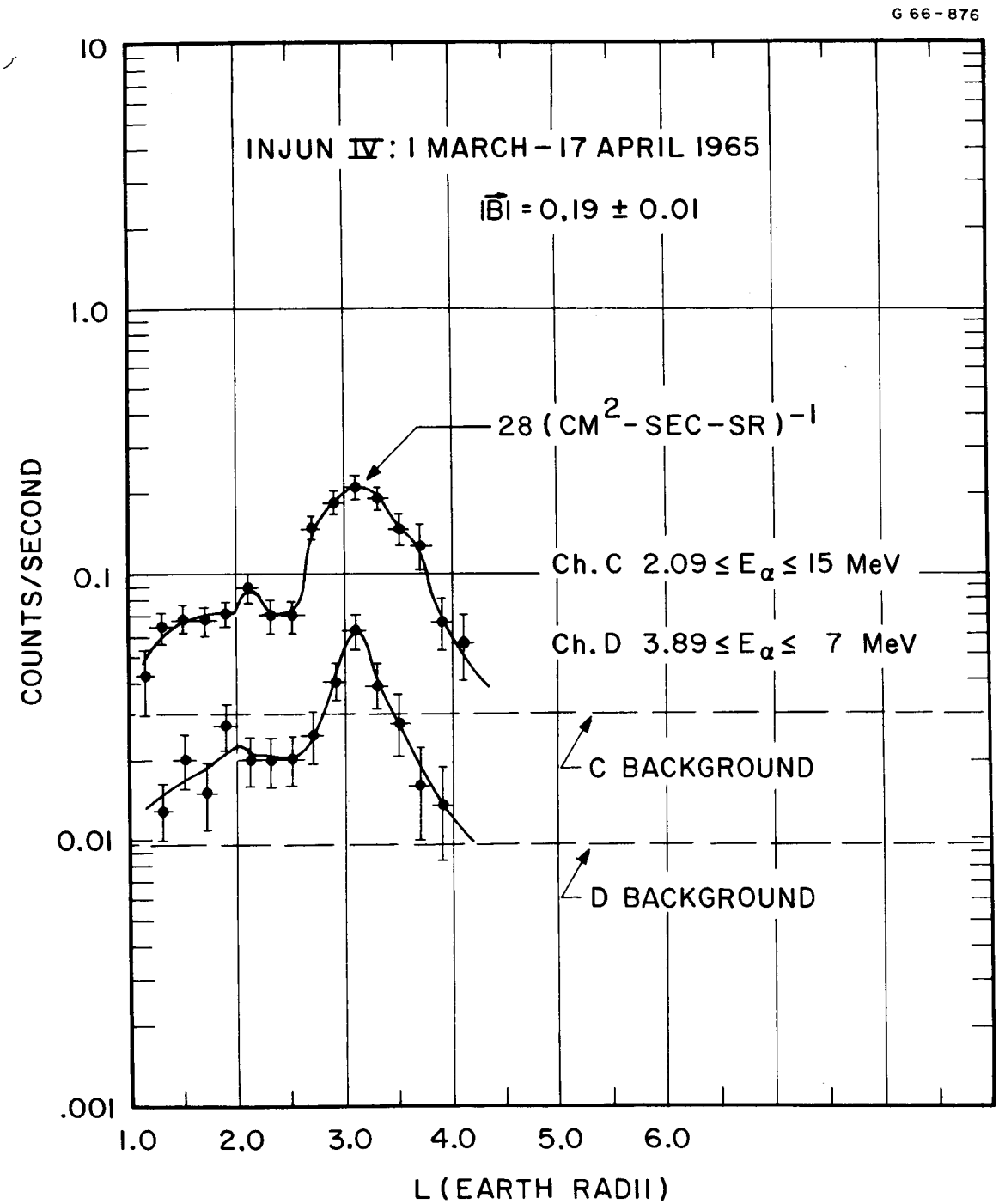
G 66-876
INJUN IV: 1 MARCH - 17 APRIL 1965
|B| = 0.19 ± 0.01
28 (CM^2-SEC-SR)$^{-1}$
Ch. C 2.09 ≤ E_α ≤ 15 MeV
Ch. D 3.89 ≤ E_α ≤ 7 MeV
C BACKGROUND
D BACKGROUND
COUNTS/SECOND
10
1.0
0.1
0.01
.001
1.0
2.0
3.0
4.0
5.0
6.0
L (EARTH RADII)

FIGURE 3

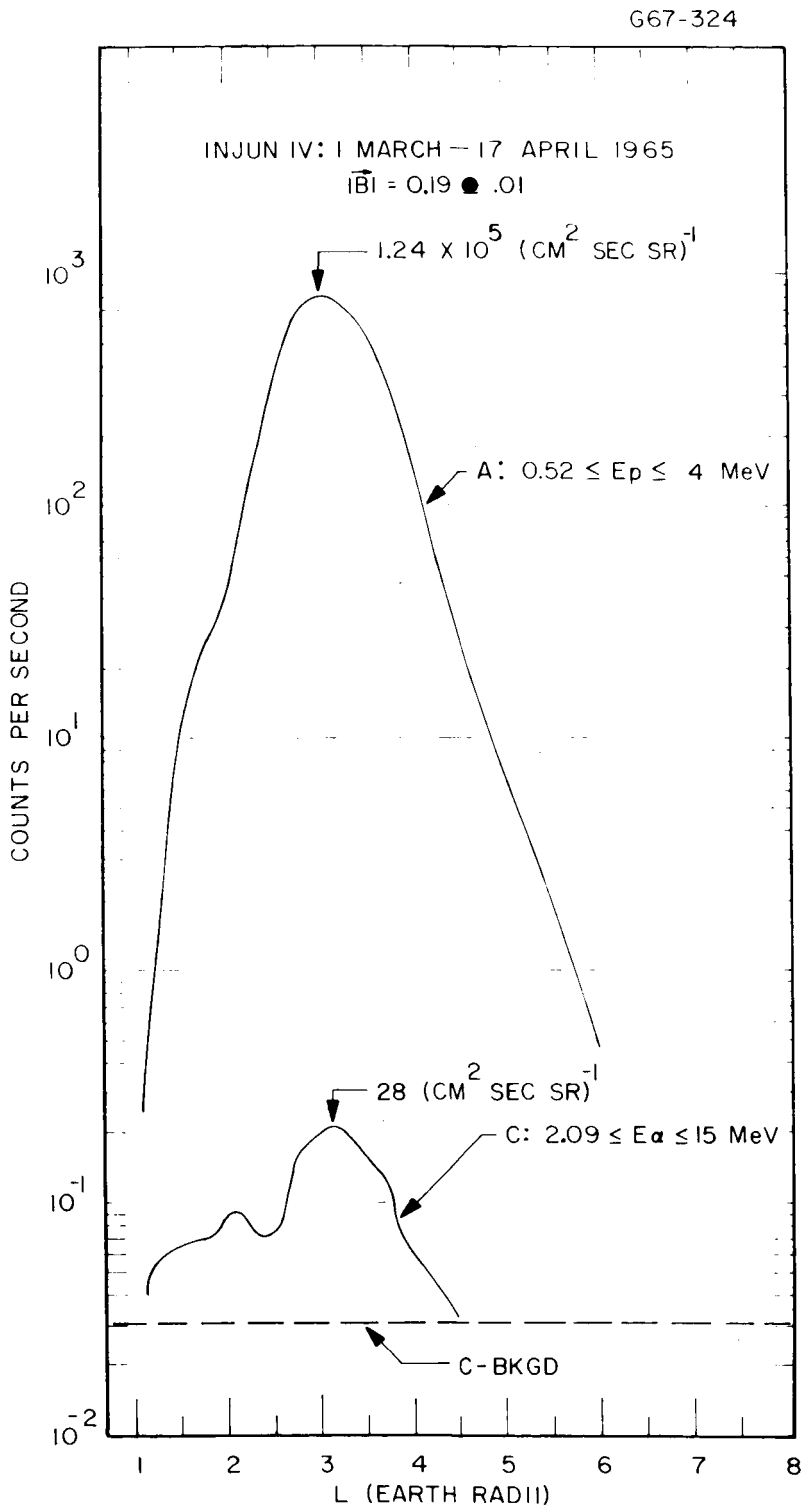
G67-324
INJUN IV: 1 MARCH – 17 APRIL 1965
|B| = 0.19 ● .01
1.24 X 10^5 (CM^2 SEC SR)^-1
A: 0.52 ≤ Ep ≤ 4 MeV
28 (CM^2 SEC SR)^-1
C: 2.09 ≤ Eα ≤ 15 MeV
C-BKGD
COUNTS PER SECOND
10^3
10^2
10^1
10^0
10^-1
10^-2
1
2
3
4
5
6
7
8
L (EARTH RADII)

FIGURE 4

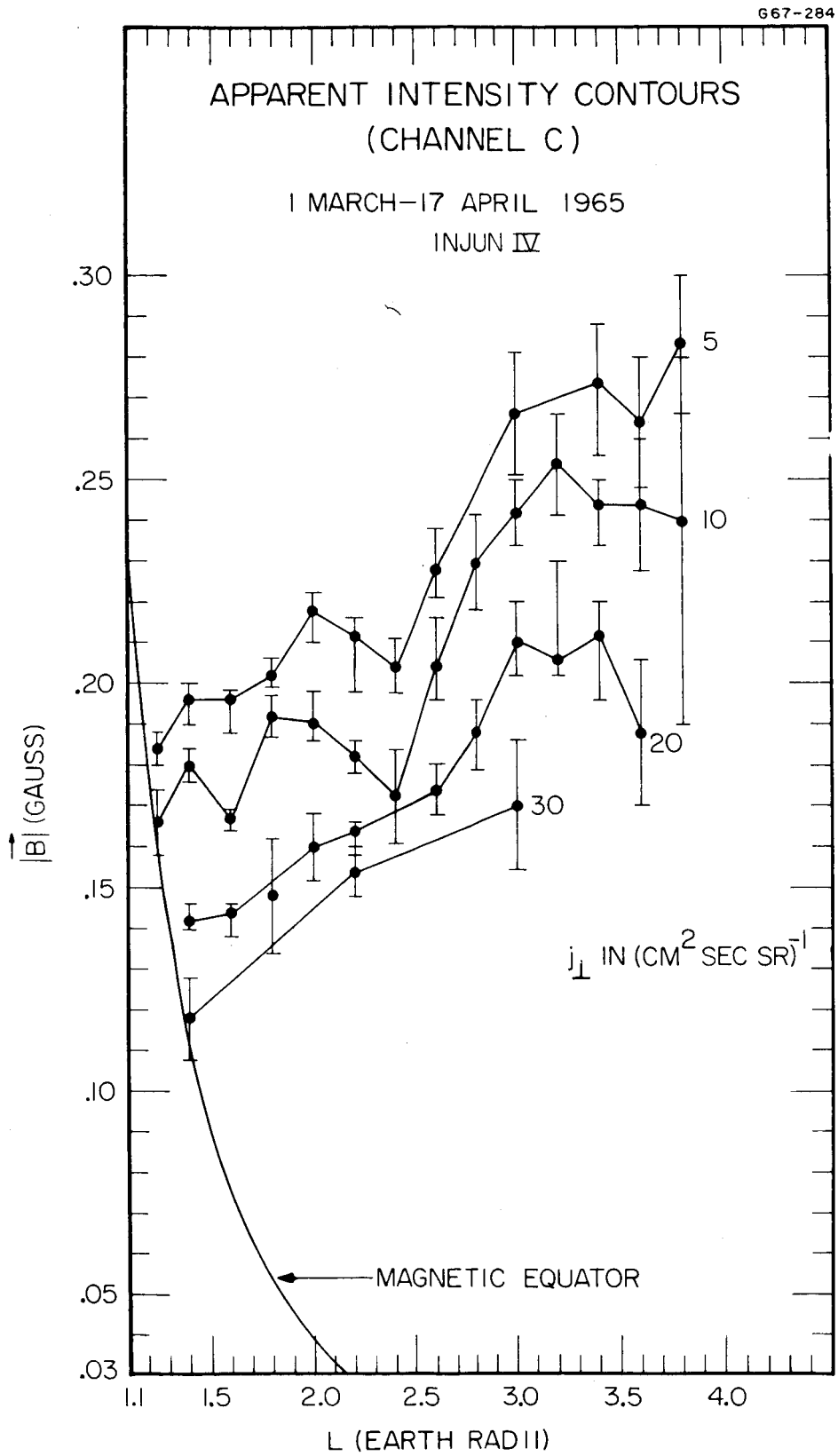
G67-284
APPARENT INTENSITY CONTOURS
(CHANNEL C)
1 MARCH–17 APRIL 1965
INJUN IV
.30
.25
.20
.15
.10
.05
.03
|B| (GAUSS)
5
10
20
30
$j_\perp$ IN (CM^2 SEC SR)$^{-1}$
MAGNETIC EQUATOR
1.1
1.5
2.0
2.5
3.0
3.5
4.0
L (EARTH RADII)

Figure 5

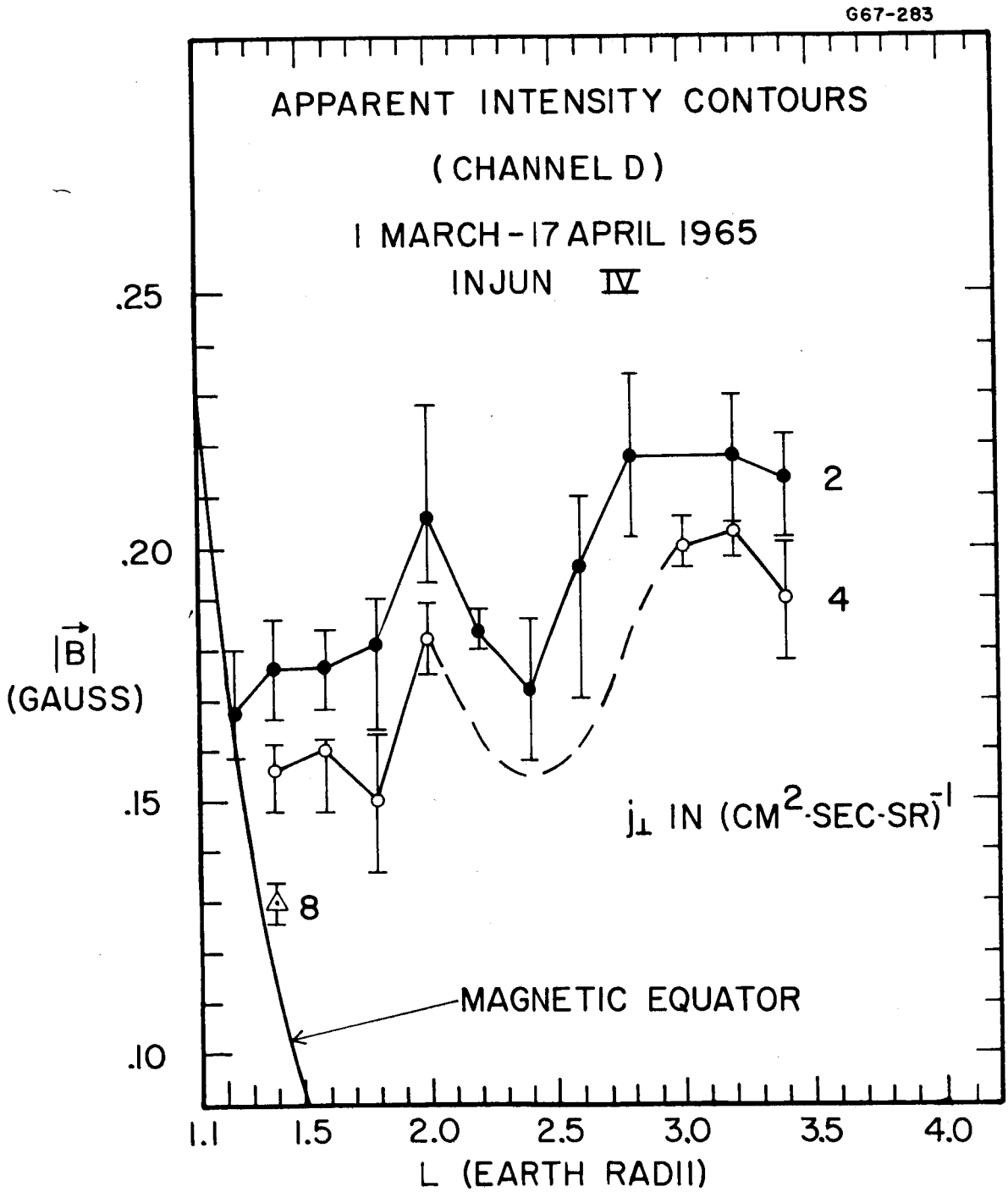
G67-283
APPARENT INTENSITY CONTOURS
(CHANNEL D)
1 MARCH - 17 APRIL 1965
INJUN IV
.25
.20
.15
.10
|B| (GAUSS)
2
4
8
j⊥ IN (CM²·SEC·SR)⁻¹
MAGNETIC EQUATOR
1.1
1.5
2.0
2.5
3.0
3.5
4.0
L (EARTH RADII)

Figure 6

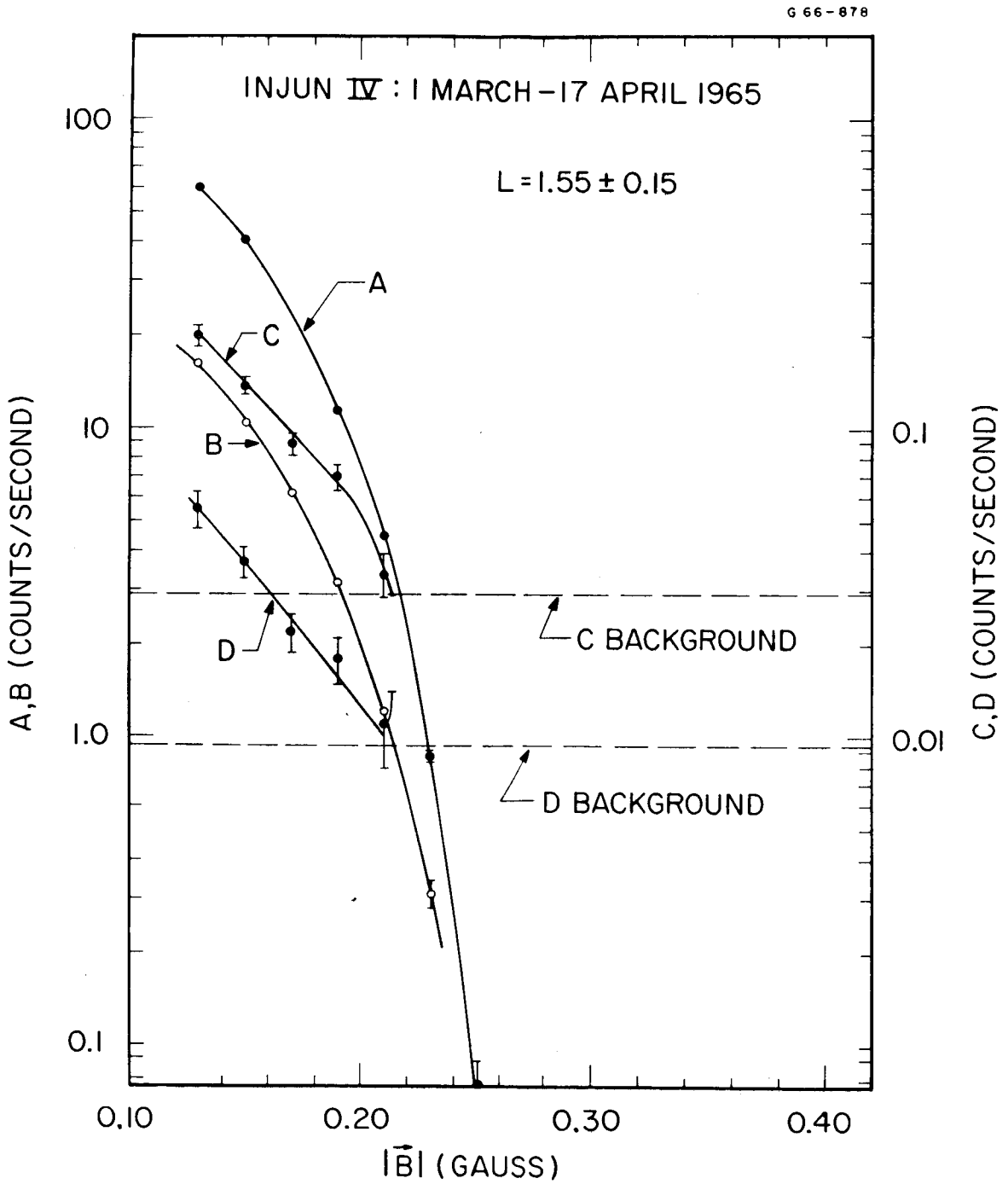
G 66-878
INJUN IV : 1 MARCH – 17 APRIL 1965
L = 1.55 ± 0.15
A
C
B
D
C BACKGROUND
D BACKGROUND
100
10
1.0
0.1
0.1
0.01
0.10
0.20
0.30
0.40
A,B (COUNTS/SECOND)
C,D (COUNTS/SECOND)
|B| (GAUSS)

Figure 7

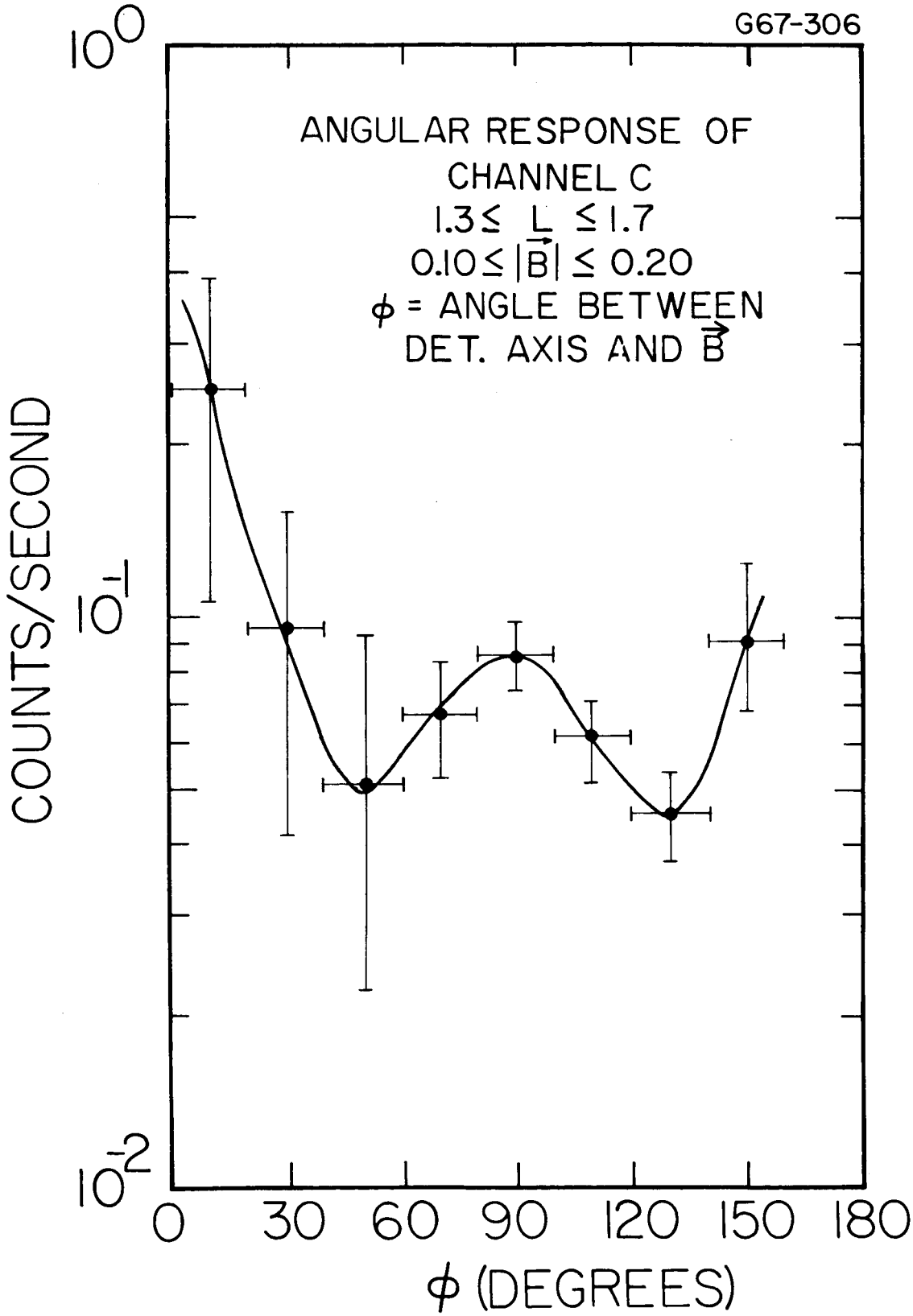
G67-306
ANGULAR RESPONSE OF
CHANNEL C
1.3 ≤ L ≤ 1.7
0.10 ≤ |B| ≤ 0.20
φ = ANGLE BETWEEN
DET. AXIS AND B
COUNTS/SECOND
10^0
10^-1
10^-2
0
30
60
90
120
150
180
φ (DEGREES)

Figure 8

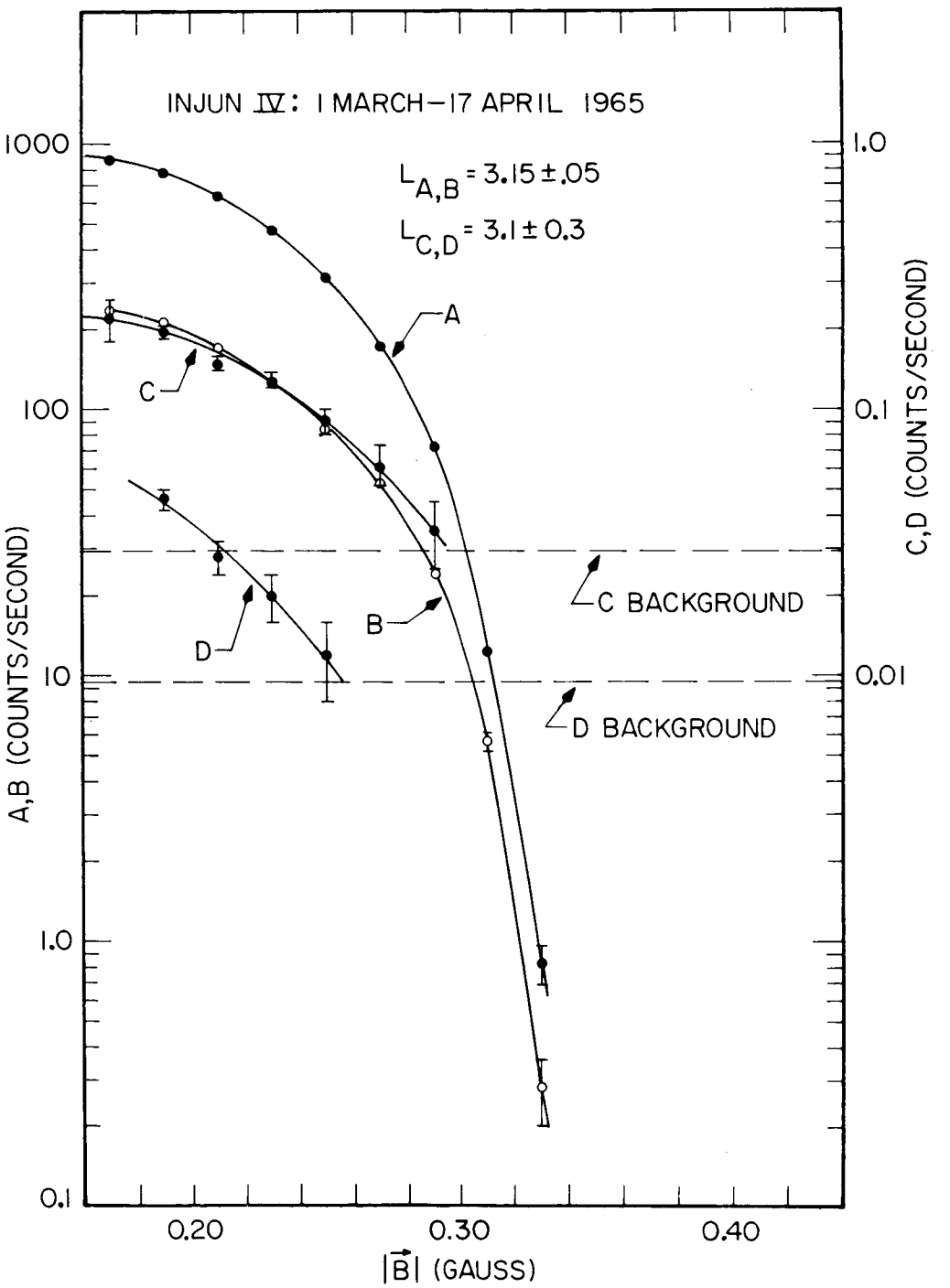
INJUN IV: 1 MARCH–17 APRIL 1965
$L_{A,B} = 3.15 \pm .05$
$L_{C,D} = 3.1 \pm 0.3$
A
C
B
D
C BACKGROUND
D BACKGROUND
1000
100
10
1.0
0.1
1.0
0.1
0.01
A,B (COUNTS/SECOND)
C,D (COUNTS/SECOND)
0.20
0.30
0.40
$|\vec{B}|$ (GAUSS)

Figure 9

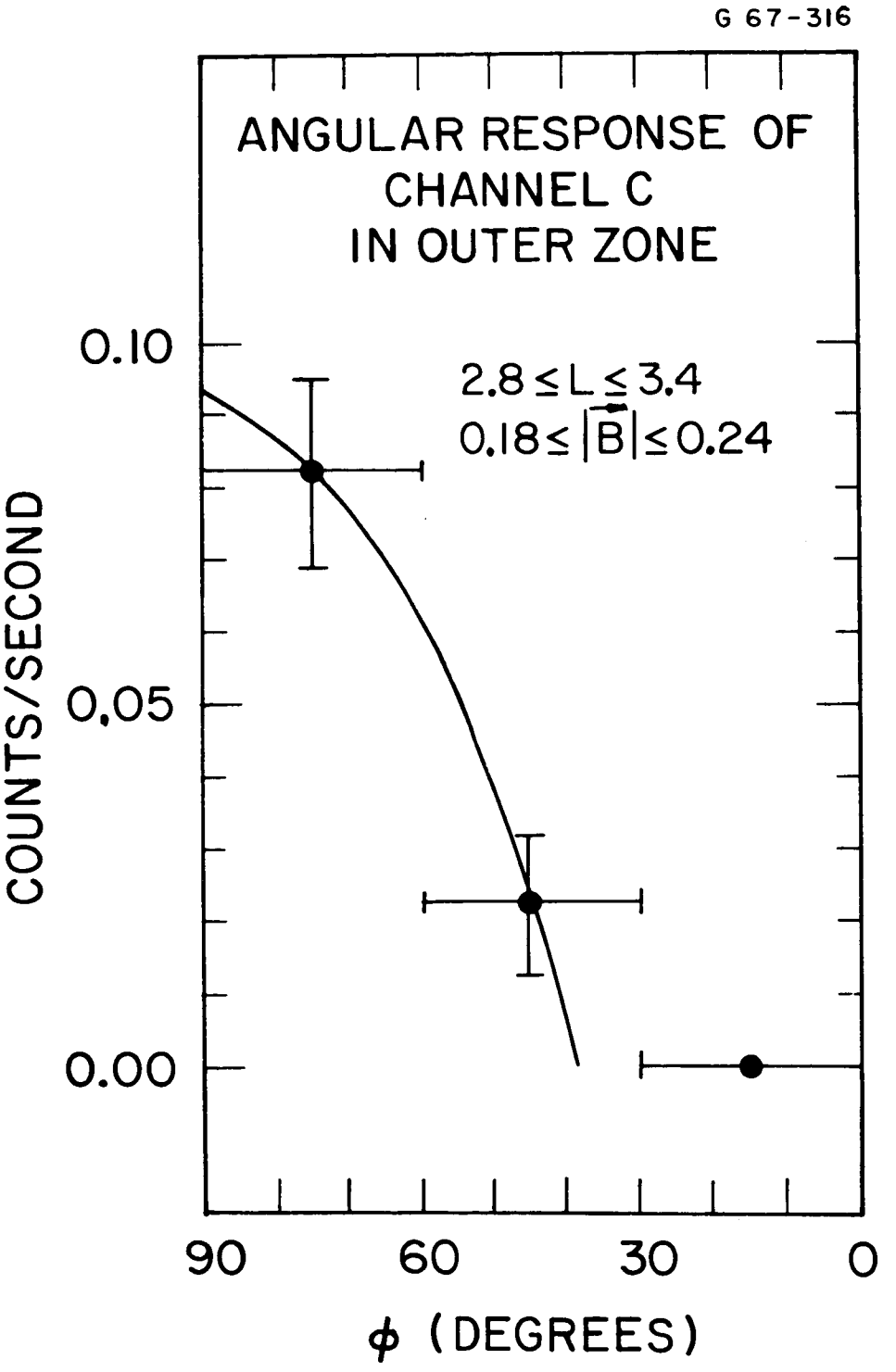
G 67-316
ANGULAR RESPONSE OF
CHANNEL C
IN OUTER ZONE
2.8 ≤ L ≤ 3.4
0.18 ≤ |B| ≤ 0.24
0.10
0.05
0.00
COUNTS/SECOND
90
60
30
0
φ (DEGREES)

FIGURE 10

G67-474

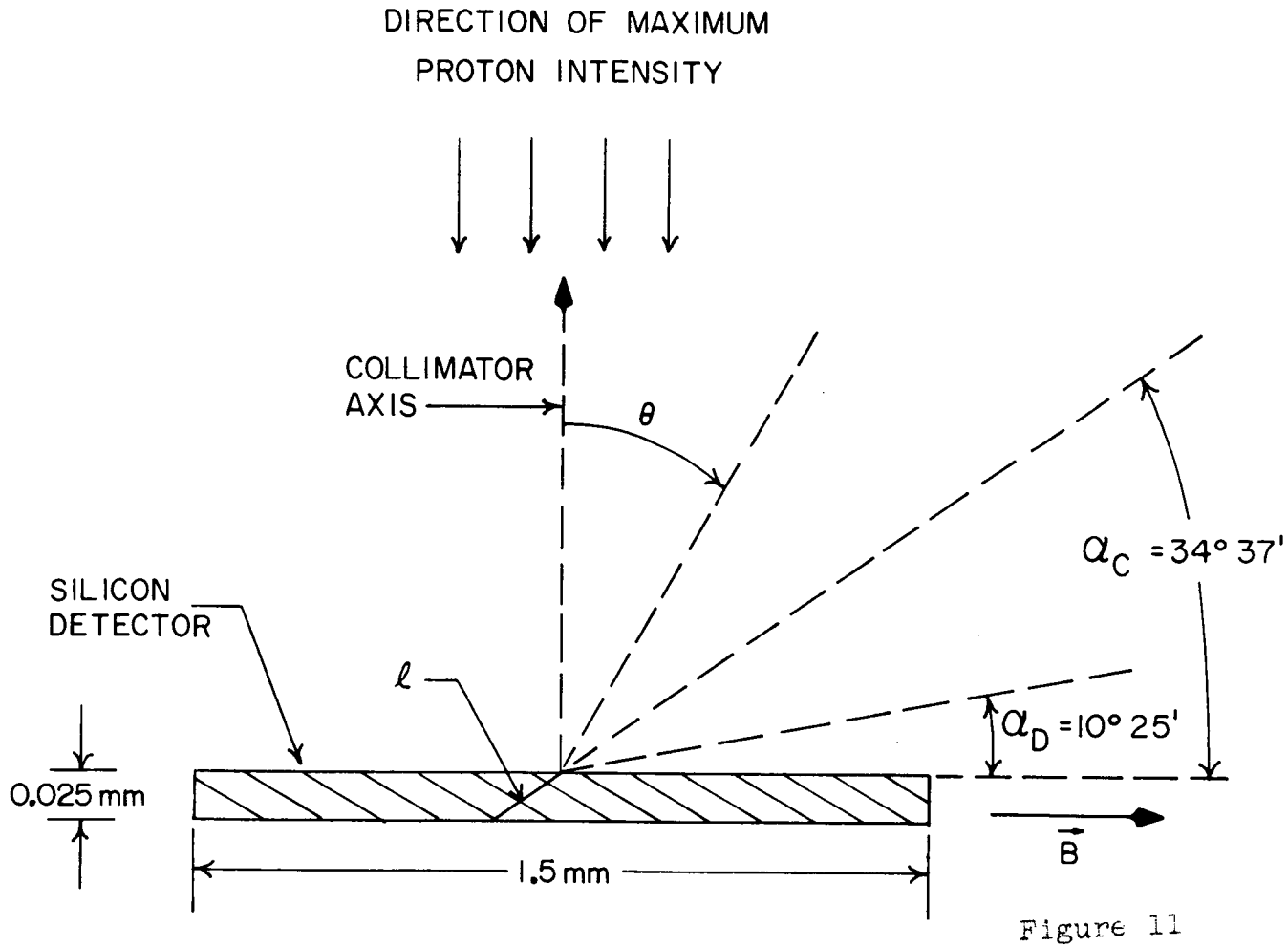

Figure 11

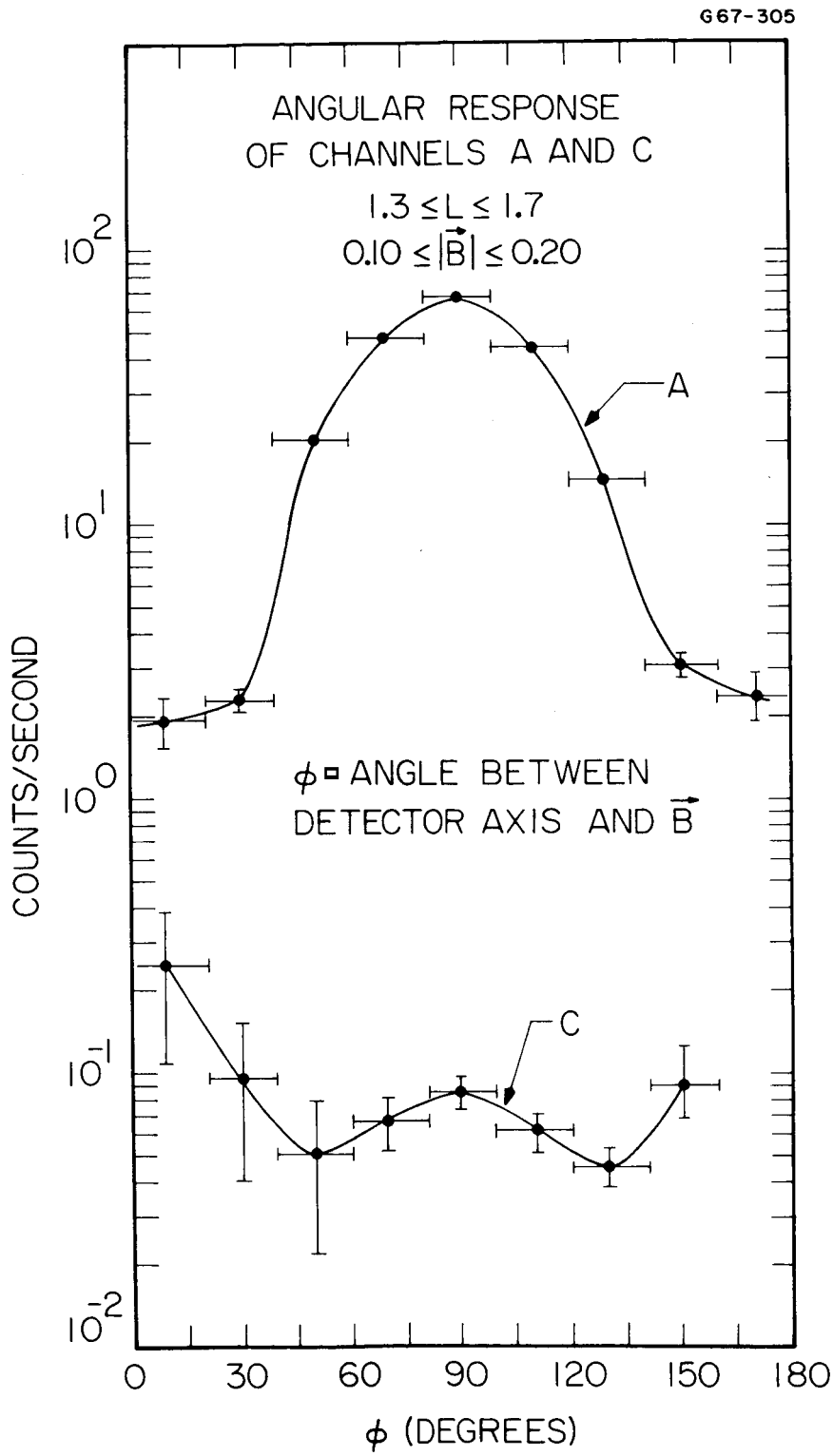
G67-305
ANGULAR RESPONSE
OF CHANNELS A AND C
1.3 ≤ L ≤ 1.7
0.10 ≤ |B| ≤ 0.20
A
C
φ = ANGLE BETWEEN
DETECTOR AXIS AND B
COUNTS/SECOND
10^2
10^1
10^0
10^-1
10^-2
0
30
60
90
120
150
180
φ (DEGREES)

Figure 12

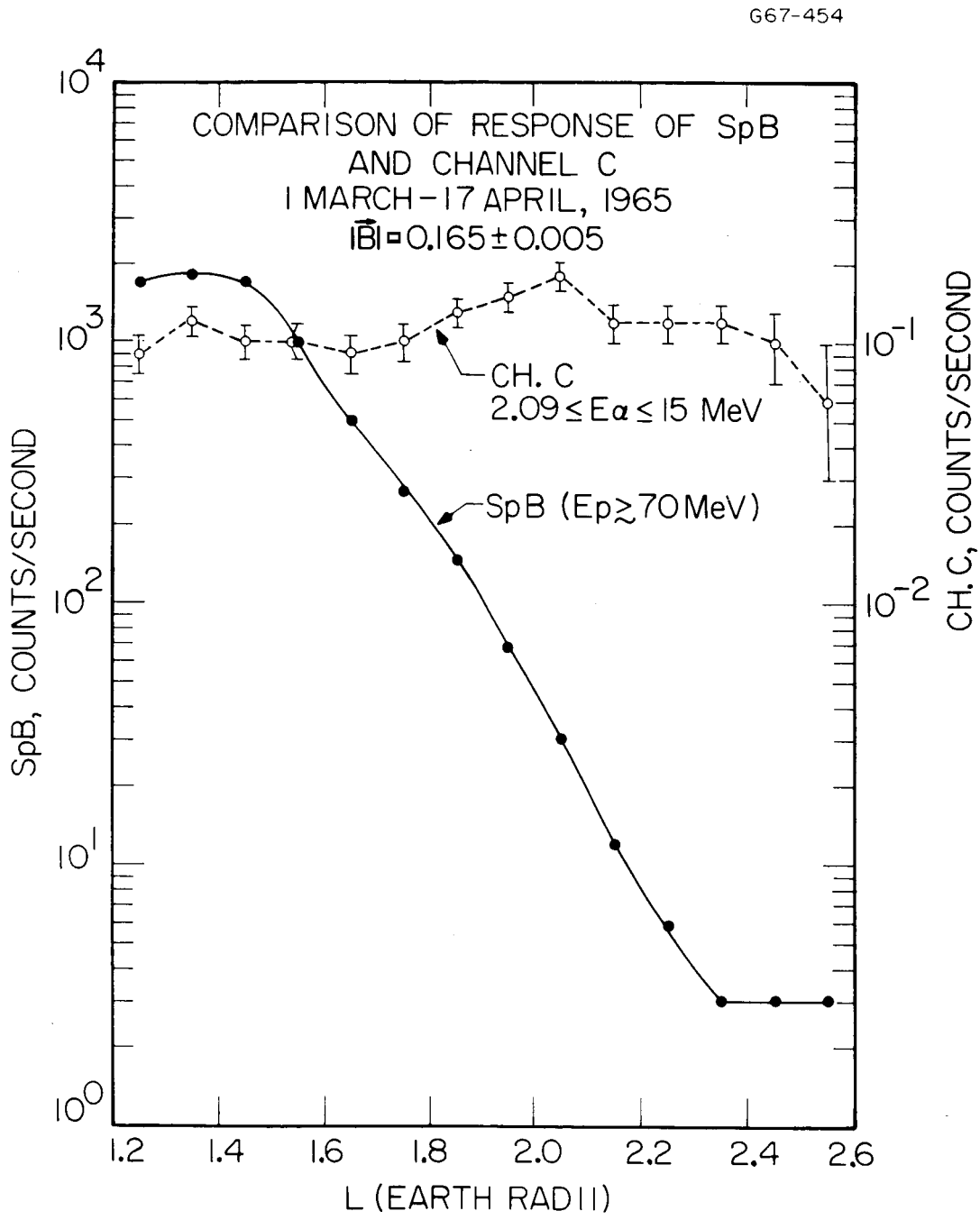
G67-454
COMPARISON OF RESPONSE OF SpB
AND CHANNEL C
1 MARCH – 17 APRIL, 1965
|B| = 0.165 ± 0.005
CH. C
2.09 ≤ Eα ≤ 15 MeV
SpB (Ep ≳ 70 MeV)
SpB, COUNTS/SECOND
CH. C, COUNTS/SECOND
L (EARTH RADII)
10^4
10^3
10^2
10^1
10^0
10^-1
10^-2
1.2
1.4
1.6
1.8
2.0
2.2
2.4
2.6

FIGURE 13

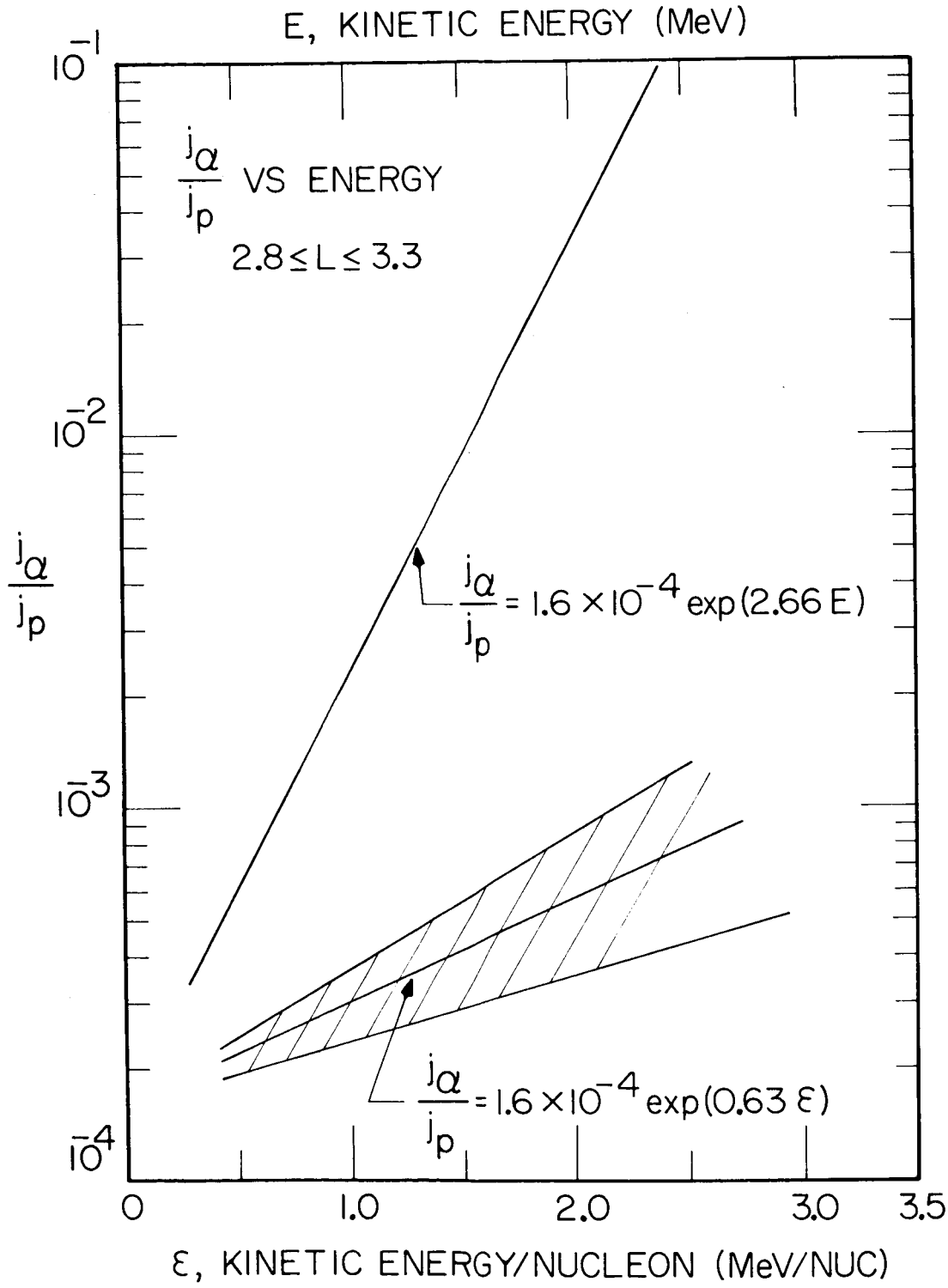
E, KINETIC ENERGY (MeV)
10^{-1}
10^{-2}
10^{-3}
10^{-4}
$\frac{j_\alpha}{j_p}$ VS ENERGY
$2.8 \leq L \leq 3.3$
$\frac{j_\alpha}{j_p}$
$\frac{j_\alpha}{j_p} = 1.6 \times 10^{-4} \exp(2.66\,E)$
$\frac{j_\alpha}{j_p} = 1.6 \times 10^{-4} \exp(0.63\,\mathcal{E})$
0
1.0
2.0
3.0
3.5
$\mathcal{E}$, KINETIC ENERGY/NUCLEON (MeV/NUC)

Figure 14

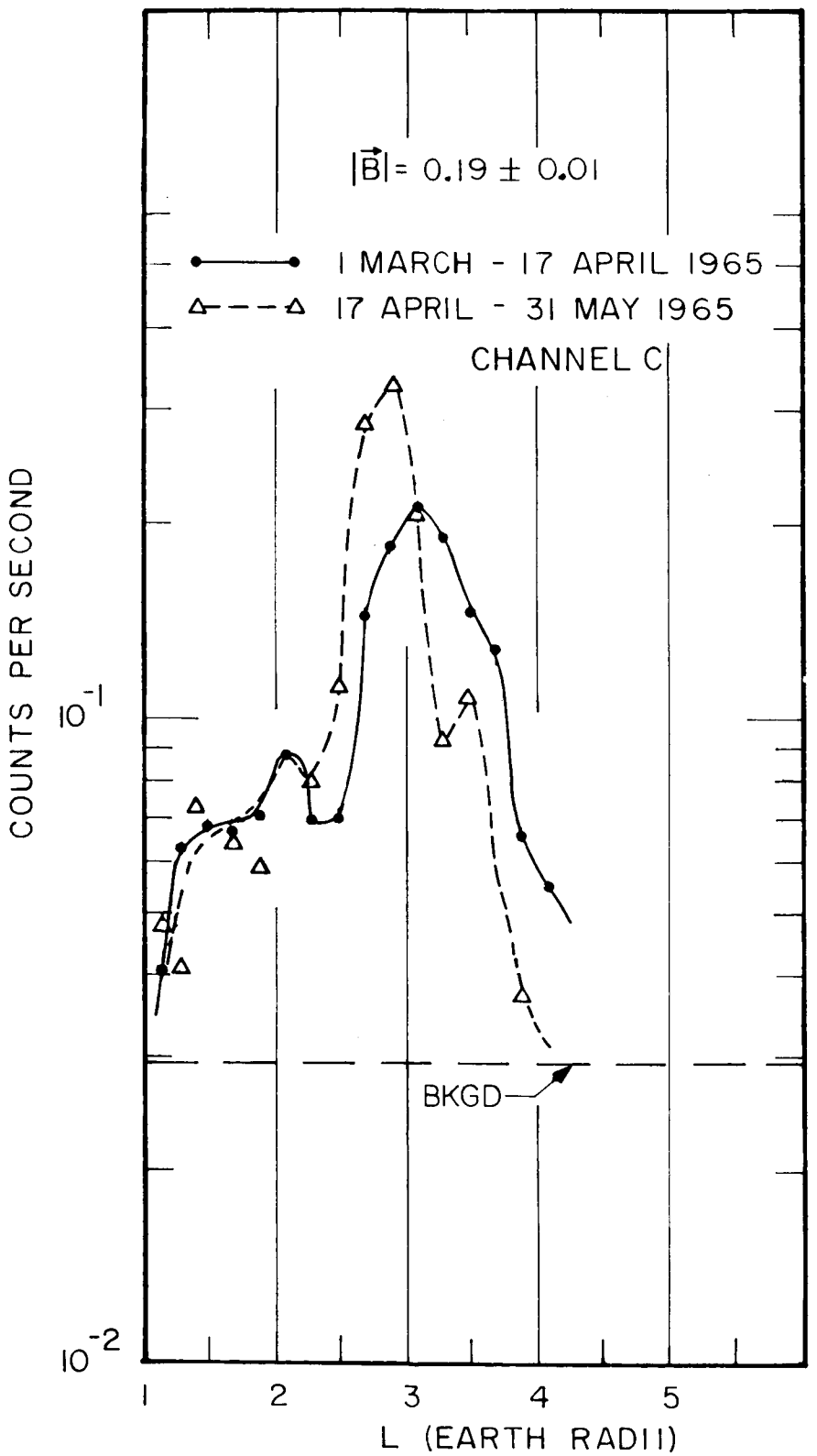
$|\vec{B}| = 0.19 \pm 0.01$
1 MARCH - 17 APRIL 1965
17 APRIL - 31 MAY 1965
CHANNEL C
COUNTS PER SECOND
10^{-1}
10^{-2}
BKGD
1
2
3
4
5
L (EARTH RADII)

Figure 15

DOCUMENT CONTROL DATA - R&D

(Security classification of title, body of abstract and indexing annotation must be entered when the overall report is classified)

1. ORIGINATING ACTIVITY (Corporate author)
University of Iowa
Department of Physics and Astronomy

2a. REPORT SECURITY CLASSIFICATION
UNCLASSIFIED

2b. GROUP

3. REPORT TITLE
Geomagnetically Trapped Alpha Particles

4. DESCRIPTIVE NOTES (Type of report and inclusive dates)
Progress July 1967

5. AUTHOR(S) (Last name, first name, initial)
Krimigis, S. M., and Van Allen, J. A.

6. REPORT DATE
July 1967

7a. TOTAL NO. OF PAGES
70

7b. NO. OF REFS
36

8a. CONTRACT OR GRANT NO.
Nonr 1509(06)

b. PROJECT NO.

c.

d.

9a. ORIGINATOR'S REPORT NUMBER(S)
U. of Iowa 67-29

9b. OTHER REPORT NO(S) (Any other numbers that may be assigned this report)

10. AVAILABILITY/LIMITATION NOTICES
Distribution of this document is unlimited.

11. SUPPLEMENTARY NOTES

12. SPONSORING MILITARY ACTIVITY
Office of Naval Research

13. ABSTRACT

The observations reported herein were made with the University of Iowa Injun IV satellite which was launched on 21 November 1964 into a nearly polar orbit of 81° inclination with initial apogee and perigee altitudes of 2502 and 527 kilometers, respectively. It carried a 25 micron thick, totally depleted silicon surface barrier detector with four electronic discrimination levels. The two levels are sensitive to protons $0.52 \leq E_p \leq 4.2$ MeV and $0.90 \leq E_p \leq 2.1$ MeV, respectively. The two upper levels are sensitive only to nuclei heavier than deuterons and, specifically, are sensitive to alpha particles $2.09 \leq E_\alpha \leq 15$ MeV and $3.89 \leq E_\alpha \leq 7$ MeV, respectively. Study of the available data up to 17 April 1965 leads to the following conclusions:

(a) The presence of geomagnetically trapped alpha particles is established.

(b) At constant $|\vec{B}| \approx 0.19$ gauss the maximum intensity perpendicular to $\vec{B}$ occurs at L = 3.1. The absolute directional intensity there is

$$j_\alpha (E_\alpha > 2.09 \text{ MeV}) = 28 \ (\text{cm}^2 \text{ sec sr})^{-1} \text{ and}$$
$$j_\alpha (E_\alpha > 3.89 \text{ MeV}) = 4.5 \ (\text{cm}^2 \text{ sec sr})^{-1}.$$

(c) At this outer zone maximum, the ratio of the directional intensities of alpha particles and of protons, both integrated above the common value $\mathcal{E}_\alpha = \mathcal{E}_p = 0.52$ MeV/nucleon, is

(continued)

DD FORM 1 JAN 64 1473

14. KEY WORDS	LINK A		LINK B		LINK C	
	ROLE	WT	ROLE	WT	ROLE	WT
Radiation Belts						
Alpha Particles						
Geomagnetically Trapped Radiation						

INSTRUCTIONS

1. ORIGINATING ACTIVITY: Enter the name and address of the contractor, subcontractor, grantee, Department of Defense activity or other organization *(corporate author)* issuing the report.

2a. REPORT SECURITY CLASSIFICATION: Enter the overall security classification of the report. Indicate whether "Restricted Data" is included. Marking is to be in accordance with appropriate security regulations.

2b. GROUP: Automatic downgrading is specified in DoD Directive 5200.10 and Armed Forces Industrial Manual. Enter the group number. Also, when applicable, show that optional markings have been used for Group 3 and Group 4 as authorized.

3. REPORT TITLE: Enter the complete report title in all capital letters. Titles in all cases should be unclassified. If a meaningful title cannot be selected without classification, show title classification in all capitals in parenthesis immediately following the title.

4. DESCRIPTIVE NOTES: If appropriate, enter the type of report, e.g., interim, progress, summary, annual, or final. Give the inclusive dates when a specific reporting period is covered.

5. AUTHOR(S): Enter the name(s) of author(s) as shown on or in the report. Enter last name, first name, middle initial. If military, show rank and branch of service. The name of the principal author is an absolute minimum requirement.

6. REPORT DATE: Enter the date of the report as day, month, year; or month, year. If more than one date appears on the report, use date of publication.

7a. TOTAL NUMBER OF PAGES: The total page count should follow normal pagination procedures, i.e., enter the number of pages containing information.

7b. NUMBER OF REFERENCES: Enter the total number of references cited in the report.

8a. CONTRACT OR GRANT NUMBER: If appropriate, enter the applicable number of the contract or grant under which the report was written.

8b, 8c, & 8d. PROJECT NUMBER: Enter the appropriate military department identification, such as project number, subproject number, system numbers, task number, etc.

9a. ORIGINATOR'S REPORT NUMBER(S): Enter the official report number by which the document will be identified and controlled by the originating activity. This number must be unique to this report.

9b. OTHER REPORT NUMBER(S): If the report has been assigned any other report numbers *(either by the originator or by the sponsor)*, also enter this number(s).

10. AVAILABILITY/LIMITATION NOTICES: Enter any limitations on further dissemination of the report, other than those imposed by security classification, using standard statements such as:

(1) "Qualified requesters may obtain copies of this report from DDC."

(2) "Foreign announcement and dissemination of this report by DDC is not authorized."

(3) "U. S. Government agencies may obtain copies of this report directly from DDC. Other qualified DDC users shall request through _____."

(4) "U. S. military agencies may obtain copies of this report directly from DDC. Other qualified users shall request through _____."

(5) "All distribution of this report is controlled. Qualified DDC users shall request through _____."

If the report has been furnished to the Office of Technical Services, Department of Commerce, for sale to the public, indicate this fact and enter the price, if known.

11. SUPPLEMENTARY NOTES: Use for additional explanatory notes.

12. SPONSORING MILITARY ACTIVITY: Enter the name of the departmental project office or laboratory sponsoring *(paying for)* the research and development. Include address.

13. ABSTRACT: Enter an abstract giving a brief and factual summary of the document indicative of the report, even though it may also appear elsewhere in the body of the technical report. If additional space is required, a continuation sheet shall be attached.

It is highly desirable that the abstract of classified reports be unclassified. Each paragraph of the abstract shall end with an indication of the military security classification of the information in the paragraph, represented as *(TS), (S), (C), or (U)*.

There is no limitation on the length of the abstract. However, the suggested length is from 150 to 225 words.

14. KEY WORDS: Key words are technically meaningful terms or short phrases that characterize a report and may be used as index entries for cataloging the report. Key words must be selected so that no security classification is required. Identifiers, such as equipment model designation, trade name, military project code name, geographic location, may be used as key words but will be followed by an indication of technical context. The assignment of links, roles, and weights is optional.

$$j_\alpha/j_p = (2.3 \pm 0.2) \times 10^{-4} .$$

(d) A variety of considerations, no one of which is decisive, suggest that the most physically significant form of the spectra of alpha particles and protons may be an exponential one in terms of energy/nucleon.

(e) It appears conceivable that the observed ratio j_α/j_p may be reconcilable with a solar-wind-source of outer zone protons and alpha particles although this ratio is significantly less than that predicted from diffusion theory with known loss processes taken into account.

(f) The distribution of outer zone alpha particles was changed markedly after the magnetic storm of 18 April 1965 and the intensity peak moving inward from L = 3.1 to L = 2.9.

(g) Trapped alpha particles in the inner zone are apparently due to a different source than that for those in the outer zone.